CLIMATE-SPACE - THEME II: CROSS-ECV ACTIVITIES

ARCFRESH (ARCTIC FRESHWATER BUDGET)

Science Requirements Document (SRD)

Prime & Science Lead: Ole Baltazar Andersen

DTU Space, Copenhagen, Denmark

Technical Officer: Anna Maria Trofaier

ESA ECSAT, Didcot, United Kingdom

Consortium:

DTU-Space, Department of Geodynamics (DTU)

ENVironmental Earth Observation IT GmbH (ENVEO)

Science and Technology AS (S&T)

Environment and Climate Change Canada Governmental (ECCC)

Norwegian Meteorological Institute (METNO)

Nansen Environmental and Remote Sensing Center (NERSC)

Norwegian Research Centre AS (NORCE)

National Physical Laboratory (NPL)

Swedish Meteorological and Hydrological Institute (SMHI)

University of Western Brittany (UBO)

Signatures page

Prepared by	Nicolas Kolodziejczyk Lead Author, UBO	Nicolas Kolodziejczyk
Issued by	Daniele Fantin, Project Manager, S[&]T	Digitally signed by Daniele Fantin Date: 2025.06.03 14:21:58 CEST
Checked by	Ole Baltazar Andersen Science Leader, DTU-S	Ole Baltazar Andersen
Approved by	Anna Maria Trofaier ESA Technical Officer	Anna Maria Trofaier Digitally signed by Anna Maria Trofaier Date: 2025.07.15 09:28:01 +01'00'

Table of Contents

Change Log

Issue	Author	Affected Se	Change	Status
0.5	D. Fantin, S&T	All	Document created	
1.0	N.Kolodziejczyk UBO	All,	Finalization of the document	Delivered to ESA

Acronyms and Abbreviations

CCI	Climate Change Initiative
CMEMS	Copernicus Marine Environment Monitoring Services
CPS	Climate Processes Section
CRD	Climate Research Division
DTU	Technical University of Denmark
ECCC	Environment and Climate Change Canada
ECV	Essential Climate Variable
ENVEO	ENVironmental Earth Observation
EO	Earth Observation
ESA	European Space Agency
FW	Freshwater
FWC	Freshwater Content
FWF	Freshwater flux
GCOS	Global Climate Observing System
GIS	Greenland Ice Sheet
GIS	Greenland Ice Sheet
GRACE	Gravity Recovery and Climate Experiment
IPCC	Intergovernmental Panel on Climate Change
IV	Ice Velocity
METNO	Norwegian Meteorological Institute
MFID	Mass Flux Ice Discharge
NERSC	Nansen Environmental and Remote Sensing Center
NORCE	Norwegian Research Centre
NPL	National Physical Laboratory
OBP	Ocean Bottom Pressure
RCM	RADARSAT Constellation Mission
S1	Sentinel-1
SAR	Synthetic Aperture RADAR
SEC	Surface Elevation Change
SIM	Sea Ice Motion
SMB	Surface Mass Balance

SMHI	Swedish Meteorological and Hydrological Institute
SoW	Statement-of-Work
SSH	Sea Surface Heights
SSS	Sea Surface Salinity
TBA	To be announced
TOPAZ	Towards an Operational Prediction system of the North Atlantic and th coastal Zone.
UBO	Université de Bretagne-Occidentale

1 Introduction

1.1 Purpose and Scope

This document contains the Science Requirements Document (SRD) for the ARCFRESH project for CLIMATE-SPACE - THEME II: CROSS-ECV ACTIVITIES, in accordance with the contract [AD1], SoW [AD2] and proposal [AD3-AD10].

The purpose of this document is to present the state-of-the-art literature on the freshwater budget and flux in the Arctic regarding the Scientific Topics (ST), including Ocean and atmospheric flux, and cryospheric and land to ocean fluxes. The document will identify the most recent advance in Arctic freshwater budget and flux monitoring and understanding, as well as the knowledge remaining gap in line with ST of the ARCFRESH project.

1.2 Document Structure

This document is structured as follows:

- Chapter 1 : Introduction
- Chapter 2 : Scientific Requirements for FW budget in the Arctic
- Chapter 3 : Scientific Requirements for EO used in the ARCFRESH project
- Chapter 4 : Uncertainty consideration and approach
- Chapter 5 : Conclusion

1.3 Applicable Documents

No	Doc. Id	Doc. Title	Date	Issue/ Revision/ Version
AD-1	4000145884/24/I-LR	ESA Contract No. 4000145884/24/I-LR	27/09/2024	NA
AD-2	ESA-EOP-SC-AMT-2023-21	Statement of Work and Annexes and Appendices	01/12/2023	1.0
AD-3	DTU-ESA-ARCFRESH-CL-001	ARCFRESH Cover Letter	22/02/2024	1.0
AD-4	DTU-ESA-ARCFRESH-TPROP-001	ARCFRESH Technical Proposal	22/02/2024	1.0
AD-5	DTU-ESA-ARCFRESH-IPROP-001	ARCFRESH Implementation Proposal	22/02/2024	1.0
AD-6	DTU-ESA-ARCFRESH-MPROP-001	ARCFRESH Management Proposal	22/02/2024	1.0
AD-7	DTU-ESA-ARCFRESH-FPROP-001	ARCFRESH Financial Proposal	22/02/2024	1.0
AD-8	DTU-ESA-ARCFRESH-CPROP-001	ARCFRESH Contractual Proposal	22/02/2024	1.0
AD-9	DTU-ESA-ARCFRESH-BF-001	ARCFRESH Background and Facilities	22/02/2024	1.0
AD-10	DTU-ESA-ARCFRESH-CV-001	ARCFRESH Curricula Vitae	22/02/2024	1.0

Note: If not provided, the reference applies to the latest released Issue/Revision/Version

2 Scientific Requirements for FW budget in the Arctic Ocean

2.1 Context

The Arctic is a pivotal region for maintaining the equilibrium of European and global climate and is itself profoundly affected by climate change. The Arctic has warmed four times faster than the rest of the globe since 1979 (Rantanen et al., 2022), leading to the amplification of the hydrological cycle associated with an increase of Freshwater (FW) flux such as precipitation and river runoff into the Arctic Ocean (*Bintanja & Selten*, 2014). The most striking feature of the "Arctic amplification" is the reduction of the Arctic sea ice cover during summer, up to 40% over recent decades (IPCC, 202; Stroeve and Notz, 2018), and acceleration of the melting of Greenland ice sheet (Bamber et al., 2012). As the Arctic transitions towards a seasonal sea ice cover, the melting season lengthens and the Marginal Ice Zone (MIZ) increases drastically (Haine and Martin, 2017). As a tracer of Freshwater (FW), ocean salinity in the Arctic is the key parameter for ocean dynamics and stratification, as well as promoting sea ice formation and shaping the ecosystem (Carmack, 2007). Therefore, the upper ocean dynamics, air-sea-ice interactions, regional climate and biogeochemical processes are also radically impacted by changes of the freshwater budget, and need to be monitored carefully (Carmack et al., 2016).

The FW budget of the Arctic Ocean plays a crucial role in global climate regulation, influencing thermohaline circulation and broader climate dynamics, by exporting FW in the global circulation. Understanding and monitoring these freshwater fluxes is essential for predicting and adapting to climate change. The FW fluxes in the Arctic Ocean contribute to the global thermohaline circulation, also known as the ocean conveyor belt (Broecker, 1997) . Changes in the FW budget can disrupt this circulation, which plays a crucial role in redistributing heat around the planet and can have cascading effects on regional and global climate patterns (IPCC, 2021). Variations in FW content influence ocean circulation patterns, including the Atlantic Meridional Overturning Circulation (AMOC), which impacts the transfer of heat between the equator and the polar regions, influencing climate conditions in adjacent areas and affecting weather patterns at lower latitudes (Rahmstorf et al., 2015).

CMIP6 models project a 40% to 60% rise in the Arctic total liquid freshwater storage at the end of this century in the SSP2-4.5 to SSP5-8.5 scenario (Wang et al., 2022), however the CMIP6 models present large bias and spreads in their FW content, suggesting ill-constrained Arctic FW processes (Wang et al., 2022). For example, the IPCC 6th assessment report highlights the need to better understand the FW input and its impacts on the global ocean circulation, such as AMOC (IPCC, 2021).

Tracing the FW cycle and an understanding of the processes associated with FW in the Arctic requires being able to address a comprehensive FW budget, including the different freshwater reservoirs on the land, in the ocean and ice, and flux exchanges between the reservoirs for any time and space varying scale.

2.2 Overview of the Arctic Freshwater system

The Arctic Ocean is a semi-enclosed basin, often called the 'Arctic Mediterranean', bordered by the large shallow (<200 m depth) Eurasian shelves on the eastern part, and deep ocean in the central part of the basin (>4000 m depth , about 50% of the surface). The Arctic Ocean represents around 1% of the global ocean volume, but receives more than 10% of the global FW river run-off (Carmack et al., 2016). Along with the Pacific Water entering the Bering Strait, the river discharges are the main supply of FW into the basin. The FW accumulates in the shallow upper layer (~200 m depth) and circulates over the warmer and saltier cyclonic circulation of the Atlantic waters that enter the Arctic on the other side of the basin through the Fram strait and through the north of the Barents Seas (Carmack et al., 2016 ; Fig. 1). The upper fresh layer is the main reservoir of FW and concentrates mainly in the upper anti-cyclonic Beaufort Gyre, while a part of the FW coming from the Eurasian Shelves are exported to the Fram Strait by the Transpolar Drift (Fig. 2.1).

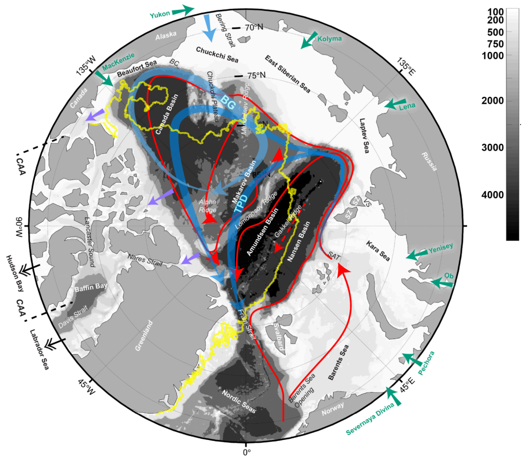

Figure 2.1: Map of the Arctic Ocean topography and main fresh and cold upper (blue arrows) and warm and salty Atlantic intermediate (red arrows) ocean currents. The main river mouths are indicated in green arrows and the main inflow/outflow in the main Arctic strait. The 2020 minimum sea ice edge is superimposed in yellow. BG : Beaufort Gyre; TPD : Trans-polar drift ; BC : Barrow Canyon ; CAA : Canadian archipelago ; and SAT : St Anna Trough (from Solomon et al., 2021).

The upper freshwater reservoir is thus separated from the intermediate salty water by the sharp halocline that is characterized by a strong vertical gradient of salinity that mainly drives the upper Arctic stratification. In the literature, many authors acknowledge the fact that density horizontal and vertical distribution in the Arctic is mainly salinity driven, referring it to a so-called “beta” ocean, given the relatively cold and homogenous temperature and the lower thermal expansion coefficient than in the "alpha" ocean, mainly driven by temperature gradients (e.g. Carmack et al.,2007). As a consequence, the salinity is the main dynamical ocean variable; thus the dynamic high and steric level change is closely related to the FW content of the Arctic upper basin (e.g. Giles et al.,2012 ; Proshutinsky et al., 2009 ; McPhee et al., 2009 : Morrison et al., 2012).

2.3 Pan-Arctic FW budget

The seminal paper by Aagård and Carmack (1989) introduced the concept of direct versus indirect methods to measure freshwater fluxes in the Arctic: the direct method measures the sum of precipitation minus evaporation plus runoff from land (rivers and glaciers), while the indirect method measures the lateral fluxes of freshwater through gateways that isolate the Arctic from the rest of the global oceans. Using mooring data (equipped with currentmeters and CTD) at gateways at Bering Strait, Davis Strait, Fram Strait and the Barents Sea Opening, the indirect method was applied by Tsubouchi et al. (2012, 2018, 2023) but limited in time to the years 2005 –2006. The freshwater flux was then estimated to 0.204 Sv, with an associated uncertainty of 0.085 Sv. That estimate was later corroborated by the analysis of in situ biogeochemical tracers (Foryan et al. 2019).

In the estimate of Haine et al. (2015) during the period 2000–2010, the Arctic Ocean stored about 101 1000 km^3 of FW (with a reference salinity to 34.8) mainly in its upper layer of a few hundred metres. On top of that, 14 300 km^3 of FW (equivalent) are stored in their solid phase as sea ice (Haine et al., 2015); a correction is made to convert a volume of sea ice to the equivalent volume of water. The upper Arctic Ocean freshwater flux is mainly fed by Riverine discharge (~4 200±420 km^3 yr^{-1}), precipitation minus evaporation (P-E) (~2 200±220 km^3 yr^{-1}) and import/export of freshwater in liquid or solid phase from gateways (2 640±100 km^3 through Bering Strait and -8 250±539 km^3 from Fram liquid and ice and Davis strait). The budget is not balanced, since a residual 1 200±730 km^3 yr^{-1} results from this estimate over the 2000 –2010 period (Haine et al., 2015). This suggests an increase of freshwater in the Arctic, which is also suggested to be the case considering a longer time period since the early 1980s (Serreze et al., 2006; Carmack et al., 2016). But it is acknowledged that there are missing terms in the budget (e.g. Greenland ice sheet, Arctic glaciers), and low confidence or incomplete mapping in the estimates of some terms of the budget (*e.g.* river runoff ; Carmack et al., 2006).

Ocean model and reanalysis can provide a consistent physical framework to estimate the FW budget. For instance, Lique et al. (2009), using a NEMO 1/12° model simulation (1965 –2002), have shown that the FW content in the Arctic is mainly controlled by the liquid FW export/import at the main gateways, except in the Fram Strait where sea ice export has also a significant contribution to FW export (Fig. 2.2). Solomon et al. (2021) has recently updated that review on Arctic FW and model based estimate (mainly Ocean-ice state reanalysis) including the years 2010 –2020 and noted the flattening of the freshwater change in the Arctic and its probable redistribution across the Arctic

Ocean, as observed in model reanalysis. As from observation, several missing FW flux terms of the budget are missing in the state-of-the-art models and reanalysis such as comprehensive river discharge estimates, Greenland ice sheet and glaciers run off (Solomon et al., 2021).

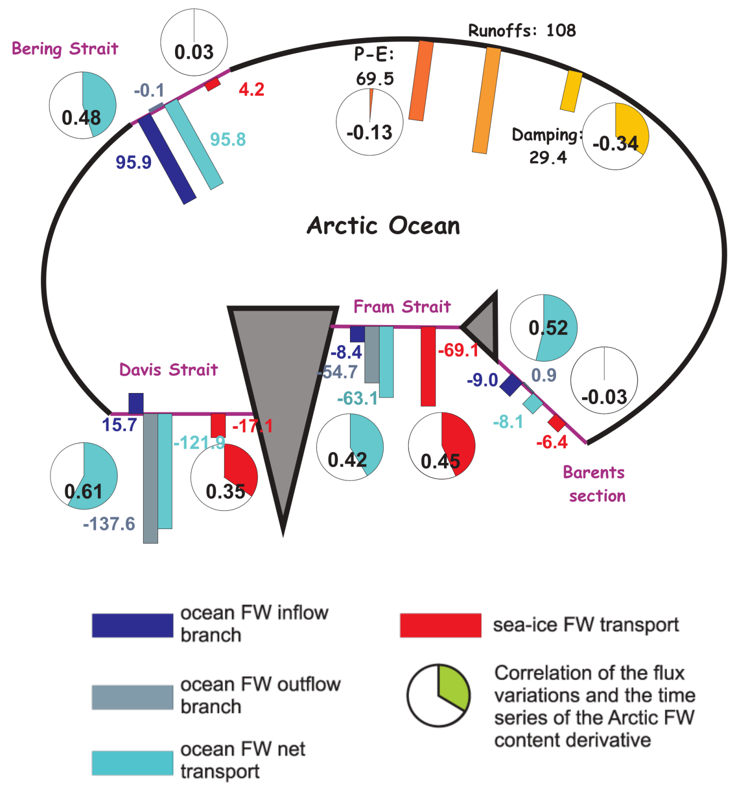

Figure 2.2 : Schematic view of the Arctic freshwater balance in an ocean/sea-ice coupled model (12 km resolution in Arctic). Mean value of each source and sink is represented (bar, in mSv), as well as the correlation of its variations with the times series of the Arctic freshwater content derivative (circular diagrams). The sign of the freshwater fluxes indicates it the flux represents a sink or a source of freshwater for the Arctic Ocean, regardless the direction of the volume fluxes (from Lique et al., 2009)

Missing terms include first a comprehensive river runoff dataset. In the Arctic, river discharge is the main freshwater supply into the small and enclosed Arctic Ocean basin (Carmak et al., 2016). River discharge has increased significantly at a rate of 15% per century over the Eurasian basin, while a weakening significant trend occurs on the North American side over a shorter period (Solomon et al., 2021; Hiyama et al., 2023; Lebedeva & Gustafsson, 2021). However, most of the Arctic is not monitored with in situ river discharge measurement stations. The Arctic Great Rivers Observatory (GRO, Shiklomanov et al., 2021) covers only 63% of the riverine discharges. Satellite observations (ESA CCI Runoff) are available for selected major rivers only, namely the Ob, Lena, MacKenzie and Collville. A consistent definition for the Terrestrial Contribution Area is to be defined as a majority of the contributing area is ungauged (Prowse et al., 2015). This renders it difficult to improve the assessment of t river runoff change and its potential impact at regional and interannual to multi-decadal scales within the Arctic Basin, as well as to quantify the significant effect it can have on Arctic Freshwater budget and export (Florindo-Lopez et al., 2020). Therefore, Le Bras and Timmermans (2025) have used routing models to derive comprehensive river runoff in the Arctic.

Other freshwater fluxes not considered previously are the Greenland ice sheet melting flux (Bamber et al., 2012), snow on sea ice and vertical redistribution (Solomon et al., 2021). They are missing in the CMIP climate models (Wang et al., 2022). Over the two last decades, the mass loss from the Greenland Ice Sheet and other Arctic glaciers that drain directly into the Arctic Ocean, have been estimated between 3% and 14% of the total mass, and have accelerated (The GlaMBIE Team., 2025). Considering the massive melting of the Arctic glaciers and Greenland ice sheet, including these fluxes will be mandatory to close a FW budget in the Arctic (Carmack et al., 2016).

Large Uncertainty in P-E flux, especially in the precipitation component has been also reported (Bromwich et al., 2018). From sea-ice coupled ocean forced model with ERA-interim fluxes, P-E has been estimated at 69.5 mSv. (Lique et al., 2009). An increase of poleward moisture transport in ERA5 data during 1979 –2018 is observed to be correlated with Arctic Oscillation (AO) index (Nygard et al., 2020). The moisture transport into the Arctic is in-phase with OA at the interannual timescale and has a positive trend (FW gain in Canadian Basin). However, large uncertainties among model reanalysis and observations and the interannual to decadal variability is poorly known (Boisvert et al. 2018).

An important missing term is the accurate estimate of the vertical mixing across the Arctic Halocline (Solomon et al., 2020). The Atlantification and reduced halocline stratification may increase vertical mixing of Atlantic water into the deep Arctic, as has occurred in the eastern Eurasian Basin where an increase of imported warm Atlantic waters and the halocline has weakened. It results in increased heat flux from below, and less beta ocean prone to sea ice formation (Carmack et al., 2016 ; Lique et al., 2015)

2.4 Regional and time varying Arctic FW

This pan-Arctic budget nevertheless hides a strong redistribution of FW at different timescales, at regional scale and also between the two main reservoirs of FW : the sea ice (solid phase) and ocean (liquid phase). At seasonal timescales, the exchange mainly occurs between the liquid/solid phase by freezing-thawing (13,400 km^3 on average over 2000-2010, Carmack et al., 2016).

The regional redistribution mainly occurs through ocean circulation forced by wind, with two main gyre systems, anticyclonic in the Canadian Basin and cyclonic in the Eurasian basin. The FW entering the Canadian basin from the Bering Strait and from the Riverine discharge on the Russian Shelves is mainly stored in the Beaufort gyre. In the Eurasian basin, the surface Trans-Polar Drift mainly transports both sea ice and liquid freshwater from the Russian shelves. Although the shelves receive large amounts of freshwater from rivers, their largest contribution to freshwater exchange comes from sea ice export (Volkov et al., 2020). The Russian Shelves freshwater volume (FWV) is ~12,574 km^3, ~16% of the Arctic Ocean, with a −15.63 km^3/year trend between 1979 and 2018. The sea ice export from the Russian Shelves (Amerasian basin) has increased by 46% (37%) over 2000-2014 compared 1998-1999 (Newton et al., 2019). Neglecting the Russian Shelf creates an error of ~25% in assessing Arctic Ocean FWV change across the 2007 regime transition (Hall et al., 2023).

The Trans-Polar Drift directly transports FW to the Fram Strait from Russian shelves. The Fram Strait is the largest sink of Arctic freshwater (sea ice export). A decrease of sea ice export detected from long-term monitoring is suspected to be due to sea ice volume loss (Smedsrud et al., 2017 ; Ricker et al., 2018; Spreen et al., 2020; Sumata et al., 2022). Sumata et al. (2023) identified a regime shift in 2007 with thinner and more uniform ice exported after 2007 compared to older and thicker multi-year ice prior to 2007 (Stern, 2025). Moreover, Krumpen et al. (2025) recently showed evidence that the Arctic sea ice is now thinner with fewer pressure ridges.

This example of redistribution of the FW between the Arctic regions to interannual timescale appears to play a crucial role in modulating the FW change in the Arctic and flux out of the Arctic (e.g. Carmack, 2016 ; Solomon, 2020). The regime shift occurring around 2007 (e.g. Polyakov et al., 2023, Sumata et al., 2023) has resulted in a step decrease (increase) of FWV on the Russian Shelf (Beaufort Gyre)(Hall et al., 2023, Fukumori et al., 2021). This interannual variability has been suspected to be caused by the atmospheric circulation through the Arctic Dipole (AD) that modulate the flow of Atlantic water from the North Atlantic across Nordic Seas, controlling the freshwater export through the Fram Strait, the import of salty Atlantic water across Barents Sea, intensify the Arctic circulation and convergence of freshwater in the Canadian basin boosting vertical stratification. Whereas AD+ leads to reduced sea ice loss, AD- increases the Arctic sea ice loss (Polyakov et al., 2023).

The FW redistribution in the Arctic may also respond to recent changes in FW flux such as Greenland melt and river discharge increase. A recent modelling study reveals, however, that recent changes in river discharge and Greenland glacier melt can contribute, with a compensation effect, to change the sea level, i.e. freshwater storage, in the Beaufort Gyre (Tajouri et al., 2024).

Climate models reveal that, sea ice decline strengthens the decadal variability of Arctic freshwater content, and the dynamics of sea level and ocean circulation (Wang, 2021). The Arctic Ocean becomes more vulnerable to winds in a warming climate, implying that extreme marine events will occur more often (Wang, 2021).

Extreme events/intra-seasonal variability are still poorly documented in the Arctic Ocean. A prime example is the role of atmospheric variability at intra-seasonal scale for driving ocean regional circulation of low salinity water such as river plumes (Taresenko et al., 2021). However, the impact on circulation and sea ice cover can have a broader effect. Parkinson et Comiso (2013) have shown the role of the September-2012 storm to reduce the Arctic sea ice cover in September to its historical minimum.

Another example is the interaction between the FW cycle and Marine heatwaves. In a warming climate, the likelihood and intensity of marine heatwaves increase (He et al., 2024). The occurrence and intensity of the marine heatwaves are intricately connected with the FW cycle, since they are shown to be driven by abrupt sea ice melting (Richaud et al., 2024 ; Borkhordarian et al., 2024). This is because the retreat of sea ice exposes the Arctic to more surface temperature variability, and change in sea ice regime may have a strong impact on the Marine heatwaves (Huang et al., 2021).

2.5 Definition of FW budget

As the ocean is salty, freshwater constitutes only a part of the seawater mass. In a water sample of 1 kg, the FW fraction of mass is simply defined as the total mass of the sample minus the dissolved matter in the sample :

$$FW = 1 - \frac{S_A}{1000} \quad (1)$$

where SA is absolute salinity in g kg^{-1} accounting for all the dissolved material in the seawater (IOC/SCOR/IAPSO, 2010). The definition is unambiguous, as it refers to the total FW content in the water sample and could be easily derived in terms of mass conservation and exchange with different reservoir containing pure FW or salt water (Schaurer and Losh, 2019).

In the literature, there is however an operational definition of “freshwater” that refers to the FW content or transport with the ocean salinity anomaly computed from a reference salinity value, following :

$$FW = \frac{S - S_{ref}}{S_{ref}} \quad (2)$$

where S_{ref} is a reference salinity and S is the measured salinity measured. This is a simple scaling to define the quantity of FW fraction added or removed from water sampled to change the salinity of the sample from S_{ref} to S. This definition presents, however, some issues extensively discussed in the literature (e.g. Schauerer and Losh, 2019). The first issue is that this definition is arbitrary and not unique in the literature, making comparison among studies difficult (e.g. Carmack et al., 2016 ; Solomon et al., 2021). Yet, generally the S_{ref} = 34.8 is widely used in the Arctic (e.g. Tsubouchi et al., 2018; Solomon et al., 2021). A second limitation is that when mass is not conserved, the FW flux will be unacceptably sensitive to S_{ref} (Tsubouchi et al., 2012).

To circumvent this ambiguous definition of FW in the context of FW budget estimation, it is thus required to come back to the use of equations of mass and salt conservation to assess the freshwater budget on a robust physical basis (e.g. Knudsen, 1900, Boyer et al., 2007, Burchard et al. 2018, Shaurer and Losh, 2019). Neglecting the variability of density and the diffusive salt fluxes through the boundary, the conservation of the mass of salt S in volume V can be written as :

$$\frac{\partial S}{\partial t} = \rho \oint_{\partial A} \int_{bot}^{top} S u_{\perp} dz dl \quad (3)$$

where S is the salinity in g.kg^{-1} ; ρ is the density, ∂A is the close contour of an elemental control volume ; $u_{\perp}$ is the perpendicular velocity to the volume ; then $Su_{\perp}$ is the salt flux across the boundary of the control volume. The conservation of salt need to be associated with volume conservation assuming that density is conserved, that can be written as:

$$\frac{\partial V}{\partial t} = \oint_{\partial A} \int_{bot}^{top} u_{\perp} dz dl + (E - P - R) \quad (4)$$

where E is evaporation, P precipitation and R stems for riverine discharge, ice sheet and glacier runoff and groundwater submarine discharge.

A more general definition of mass conservation is required in the Arctic with no assumption on constant density and encompassing both liquid freshwater and solid ice reservoir and flux is proposed by Le Bras and Timmermans (2025) :

$$\frac{d(\rho V)}{dt} = M_{OCE} + M_{SIF} + M_{FW} \quad (5)$$

where M is the net mass flux entering the control volume with subscripts being OCE for ocean flux, SIF for sea ice flux, and FW for freshwater fluxes. As above, FW flux includes precipitation, evaporation, runoff from rivers, glaciers, and groundwaters. The mass budget is differentiated with volume conservation equation :

$$\frac{d(V)}{dt} = F_{OCE} + F_{FW} + (\rho_{SI}/\rho_{ML})F_{SIF} + 0.8\,\rho_{ML}/\rho_{FW}\ 1)\,F_{SIM} \quad (6)$$

where d(V)/dt is the rate of change of the integrated volume and F represents net volume fluxes entering the control volume. In other words, changes in the integrated control volume (which is the volume of the ocean including the volume displaced by sea ice), are caused by net oceanic and freshwater fluxes entering the domain as well as sea ice fluxes and sea ice melt, scaled as detailed in Le Bras and Timmermans (2025). Finally, differentiating Equation (5) and (6) allows us retrieving the steric budget which is a good proxy for the FW budget in the Arctic (e.g. Giles et al., 2012). This approach is also well convenient in a full budget approach accounting for FW storage and fluxes, and also when using steric sea level from satellite altimeters for deriving FW content (Le Bras and Timmermans, 2025), as it will be done in the ARCFRESH project.

2.6 Control volume definition

Careful definition of the 'control volume' is important to enable a test of the closure of the FW budget in the Arctic in a robust manner. The 'control volume' is the specific volume of water that is defined as being 'Arctic Ocean'. It is defined by a surface area given through outer edge regional boundaries — both for the whole region and for subregions. The boundaries are often called 'gateways' when considered in terms of solid or liquid flux travelling across the boundary. Over the last few decades, the main gateways of the Mediterranean Arctic basin, i.e. Fram Strait, Bering Strait, Davis Strait, Barents Sea Opening (Fig. 2.3), have been equipped with mooring and glider lines in order to monitor liquid and ice water transport (e.g. Skagseth, 2008, Curry et al., 2014, Karpouzoglou et al., 2022). These observing systems have been used by Tsuboushi et al. (2012, 2018) and LeBras and Timmermans (2025) to define the boundary of the control volume for their estimates of the FW budget in the Arctic (Fig. 2.4).

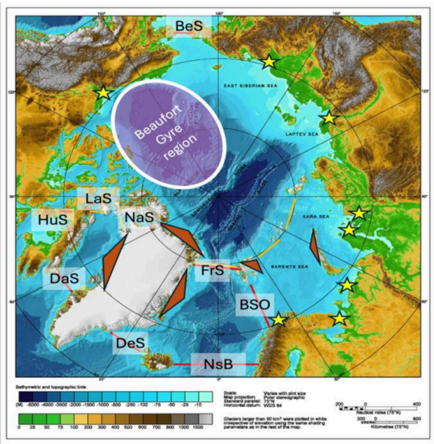

Figure 2.3: Main Arctic gateways : Lancaster Sound (LaS) ; Hudson Strait (HuS), Nares Strait (NaS), Davis Strait (DaS), Fram Strait (FrS), Bering Strait Opening (BSO), Norwegian Sea Boundary (NsB), Denmark Strait (DeS), Bering Strait (BeS).

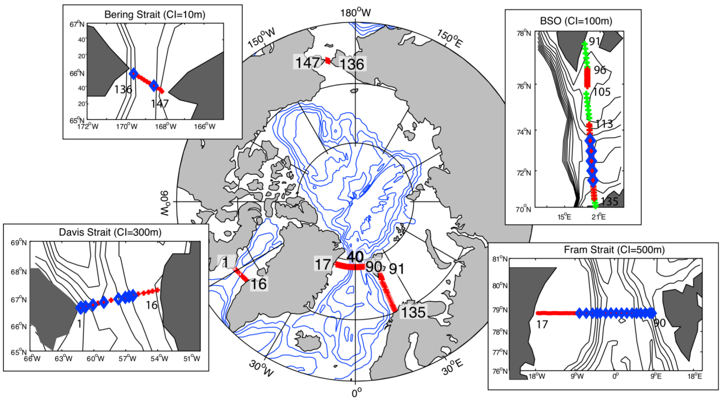

Figure 2.4: Location of mooring line across Bering Strait, Davis Strait, BSO and Fram Strait (from Tsubouchi et al., 2012).

The ocean FW budget control volume is constrained by the different components of the FW cycle in the Arctic. For example, the subdomains may account for a consistent definition for the Terrestrial Contribution Area riverine discharges (Prowse et al., 2015). Also, the Greenland sheet melting FW discharge has to be included in the FW budget control volume (Bamber et al., 2012). This is not fully compatible with the Arctic boundary definitions that account for the gauged gateways alone. Inclusion of the Nordic Seas and Norwegian Sea Boundary and Denmark Strait in the control volume is likely to lead to a better closure of the FW budget.

The FW budget closure from EO is also constrained by the availability and the quality of the satellite observations. Anderson et al. (2019) have shown that the use of geostrophic velocity computed along satellite tracks can provide longer time series at the main gateways of the Arctic basin. However, this approach likely needs to be calibrated and validated against in situ time series from the gateways mooring line. Therefore, colocated satellite tracks at the gateways are required. This consideration sets a limit on the boundaries of the control volume to match the maximum latitude of different relevant satellite orbits.

Gateway choices for sea ice export derived from satellite products are also constrained by the quality of the sea ice concentration measurements. For instance, at the Fram Strait, sea ice velocity measurements uncertainty increases with sea ice velocity (Sumata, 2015). More northward sea ice gateways (~82°N) are generally required to better assess the sea ice export into the Nordic Seas (Fig. 2.5 ; Ricker et al., 2018).

Assessing the regional FW budgets requires dividing the Arctic into subregions and using these regional definitions consistently across the different components of the budget: the liquid and solid FW reservoirs, including ice sheet and riverine discharge, sea ice dynamics and flux and ocean gateways. Regional sub-domains, delimited by either geometric boxes or by more contorted bathymetry-following box limits, compliant with the marginal seas in the Arctic domain (Barents, Kara, Laptev, East-Siberian, Chuckchi and Beaufort Seas), are generally used to use FW dynamics on the Siberian shelves (e.g. Hall et al., 2023 ; Hudson et al., 2024), Beaufort Gyre FW budget (e.g. LeBras and Timmermans, 2025), sea ice regional exchange (e.g. Ricker et al., 2018), or SSS signature from sea ice melting FW input (e.g. Van Straaten et al., 2025). Ocean gateways and subregional control volume will be defined in the Fit for Purpose documents of the ARCFRESH project (WP2).

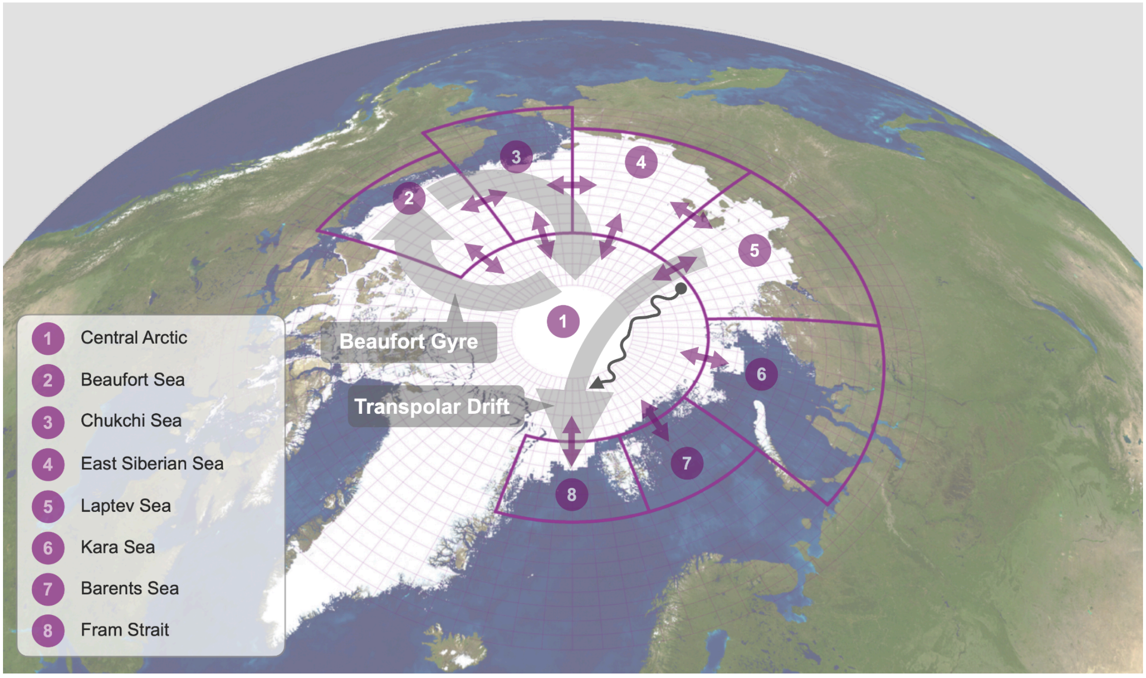

Figure 2.5: Sea Ice gateways and subregion in the Arctic, adapted from Ricker et al. (2021).

2.7 Budget requirements in the Arctic

Estimating the FW budget in the Arctic requires being able to quantify the different terms of the conservation equation within a control volume, at the different time and space scales. Thus, the freshwater budget estimate requires :

- A clear definition of the control volume or domain boundaries within which the budget is applied (Prowse et al., 2015) ;
- Acknowledging the time and space scale over which the budget is estimated ;
- Quantification of the freshwater reservoir and flux needed to close the budget.

At the pan-Arctic scale, the freshwater reservoir fluxes required for closing the budget have been identified from the literature (e.g. Haine et al., 2015; Carmack et al., 2016 ; Solomon et al., 2021) :

- Liquid reservoir: The Arctic Ocean is a semi-enclosed basin — a so-called Mediterranean type basin — with complex horizontal and vertical structure of the water masses. The main reservoir of FW is the upper, low salinity layer isolated from the deep ocean by the Halocline. FW concentrates mainly in the Beaufort Gyre region. Complex advection and mixing processes redistribute the FW within the Arctic domain (Carmack et al., 2016).
- Riverine discharges, especially on the Russian shelves, is the main source of Arctic freshwater (~11% of the global riverines discharges, Carmack et al., 2016).
- Import/export of freshwater at ocean gateways mainly from the Atlantic, bringing warm and salty water ; and from the Pacific, being the second major source of FWin the Canadian basin (Woodgate et al., 2015; Haine et al., 2015)
- Evaporation minus precipitation (E-P) that constitute the meteoric flux of FW, either liquid or solid (Carmack et al., 2016). ('Meteoric FW' refers to water that originates from rain, snow or ice melt rather than seawater or groundwater).
- Groundwater submarine discharge has been suggested to become a significant flux as FW drainage and permafrost thaw increase from the Arctic continent (Charkin et al., 2017).
- Solid reservoir : Arctic sea ice that stores about 12% of the Arctic FW (Haine et al., 2015) and ice sheets.
- Greenland ice sheet and other Arctic glaciers show an acceleration of their mass loss (e.g. The GLaMBIE group, 2025). They now need to be considered for balancing the FW budget in the Arctic (Carmack et al., 2016 ; Solomon et al., 2021), while previously they had provided only a small component of the FW budget compared to other sources.

In the next Section, from the perspective of ARCFRESH, we will review in more detail the state of the art and the knowledge gap associated with the different time series of observations and models used in the project, to address the above questions.

3 Specific scientific requirements for EO used in ARCFRESH project

3.1 Ocean models for self-consistent freshwater budget estimation

State of the art

The 5th version of the TOPAZ ice-ocean model will be used for model-based freshwater flux calculations and compare with the observation-based analysis. The model is based on the recent version 2.2.72 of the Hybrid Coordinate Ocean Model (HYCOM) coupled with the sea ice model CICE version 5.1 using the ESMF coupling software. The model is mass conserving and applied at a horizontal resolution of 6 km and with 50 hybrid z-isopycnic (constant density) vertical layers. The model input terms are the following:

- Surface fluxes from the atmosphere come from the ECMWF reanalysis ERA5, including liquid and solid precipitations. The bulk formulas for heat fluxes and evaporation-minus-precipitation are following the COARE 3.1 standards.
- Lateral boundary conditions (currents, temperature, salinity) are taken from the global Mercator Ocean International model reanalysis GLORYS at the South of the Bering Sea and across the North Atlantic between France and Newfoundland so that all of the Arctic and Greenland are fully included. The freshwater terms across the boundary will be considered as uncertain within the project.
- River discharges are composed of a several rivers taken from the following data sets:
  - The Arctic-HYPE climatology (1979-2013)
  - The E-HYPE climatology for the European Rivers included in the TOPAZ5 model domain
  - The Greenland Ice Sheet CCI data from 8 regions redistributed to the 30 largest terminal glaciers.

Scientific Requirement

A common issue in oceanography is that while models can agree on the overall trend of freshwater (FW) changes, pinpointing the specific areas of redistribution remains elusive. The discrepancy in geographical redistribution among global model reanalyses underscores the complexity of oceanic processes and the limitations of current modelling capabilities. Improving our understanding of these dynamics requires more detailed observations and enhanced models to capture the regional movements of freshwater within the Arctic Ocean system, especially in regions affected by factors like melting ice, precipitation patterns, and river discharges.

3.2 FW storage assessment

3.2.1 Sea Level

State of the Art

Sea level is a fundamental parameter for monitoring large-scale climate variability in the Arctic Ocean, as it integrates virtually all static and dynamic processes within the region's hydrosphere and atmosphere. It reflects contributions from ocean circulation, steric changes (due to temperature and salinity variations), mass inputs (e.g., freshwater from rivers, precipitation, and ice melt), and atmospheric pressure effects, making it an essential metric for understanding the Arctic's role in global climate dynamics.

Satellite altimetry missions from the European Space Agency (ESA), such as ENVISAT, CryoSat-2, and Sentinel-3, provide extensive temporal and spatial coverage of Arctic sea level, enabling detailed studies of sea level and freshwater budgets despite challenges posed by sea ice and sparse in-situ observations.

In this project, satellite-observed sea level is leveraged for two primary purposes: (1) to estimate the geostrophic balance and thereby compute volume and freshwater fluxes across ocean gates, and (2) to validate freshwater content changes by constructing a sea level budget. For the geostrophic balance calculation we use the Dynamic Ocean Topography (DOT), defined as the inverted-barometer-corrected sea surface height (SSH) relative to the geoid, which isolates the dynamic component of sea level driven by ocean currents and density gradients. DOT is derived by subtracting the geoid height from altimetry-measured SSH (see Ocean Gateways for more details).

ESA's Sea Level Climate Change Initiative (SLCCI) offers multimission data (ERS-1/2, ENVISAT, CryoSat-2, Sentinel-3) for global sea level, but excludes the Arctic due to sea ice interference and melt pond effects. The CCI Sea Level Budget dataset (Rose et al., 2019) addresses this gap, providing weekly Arctic sea level from 1996–2019 using ERS-1/2, ENVISAT, and CryoSat-2 up to 82°N.

Satellite-observed sea level, integrated with GRACE ocean bottom pressure (OBP) data, facilitates freshwater budget analysis in the Arctic by connecting steric height variations to salinity-driven freshwater content changes.

Giles et al. (2012) and Morisson et al (2012) pioneered this method in the Beaufort Gyre and pan-Arctic, using altimetry and GRACE to highlight salinity's dominant role in density shifts. Armitage et al. (2016) extended this approach, quantifying freshwater export through Fram Strait (~2000–3000 km^3/yr) from 2003 to 2014, driven by wind-induced circulation changes. Solomon et al. (2021) further refined estimates, documenting a ~7500 km^3 freshwater increase in the Arctic (2003–2008), followed by a 6000 km^3 decline (2008–2013) using the CCI Sea Level Budget dataset from Rose et al., 2019. Le

Bras and Timmermans (2025) used sea level data from Armitage et al (2016) to attribute interannual freshwater shifts (e.g., ~7500 km³ rise by 2012) to ocean fluxes, but did not find the decrease reported by Solomon et al. (2021) due to the use of a different sea level product (Rose et al, 2019 vs Armitage et al, 2016).

Knowledge gaps

The seasonal presence of sea ice severely hampers the quality and availability of sea level observations in the Arctic Ocean, making full annual mapping of variations challenging. With the exception of CryoSat-2, most satellites leave an 800 km radius "pole hole" north of ~81.5°N. Summer melt ponds on sea ice confuse low-resolution altimeters (e.g., Envisat), introducing uncertainties up to ~15 cm in sea surface height for multi-mission datasets (Rose et al., 2019). CryoSat-2's SAR altimetry cuts this to ~5 cm in ice-covered areas, thereby decreasing the uncertainty in altimetry-derived freshwater estimates by a factor of three.

The marginal ice zone (MIZ), where open water transitions to sea ice, has large uncertainity and data gaps due to differing impacts on LRM (low-resolution mode) (Enivsat) and SAR altimetry (CryoSat-2, Sentinel-3) (Rose et al., 2019). Additional gaps include limited tidal model accuracy (~5–10 cm error in shallow shelves) and geoid uncertainties, critical for DOT estimation.

3.2.2 Ocean Bottom Pressure

State-of-the-art

Ocean Bottom Pressure (OBP) is a cornerstone of Arctic ocean physics separating mass-driven sea level changes from steric effects due to temperature and salinity-driven density shifts. In the Arctic, integrating OBP with steric sea level enhances sea surface height estimates or validates altimetry observations (Ludwigsen et al., 2021), while combining altimetry-derived sea level anomalies with OBP retrieves steric height, enabling FW Content (FWC) estimates critical for budget analyses (Giles et al., 2012; Armitage et al., 2016; Solomon et al., 2021). From April 2002 to June 2017, the Gravity Recovery and Climate Experiment (GRACE) delivered quasi-monthly, Arctic-wide OBP at ~300 km resolution, succeeded by GRACE Follow-On (GRACE-FO) since July 2018. GRACE has been pivotal in mapping long-term and inter-annual FWC variability (Morison et al., 2007, 2012; Peralta-Ferriz & Morison, 2010; Peralta-Ferriz et al., 2014, 2016; Solomon et al., 2021, Le Bras and Timmermanns, 2025).

In the ARCFRESH project, GRACE-derived Ocean Bottom Pressure (OBP) and altimetry-derived sea level will quantify regional and pan-ArcticFWC to validate FWC derived from freshwater fluxes through straits and land inputs. Recently, Peralta-Ferriz and Woodgate (2023) utilized GRACE OBP alongside altimetry to estimate water transport through Bering Strait, inferring volume transport from basin-scale OBP gradients (e.g., Bering Sea to Chukchi/East Siberian Seas) rather than direct strait measurements, achieving freshwater flux estimates of ~2300–3500 km^3/yr when combined with in-situ salinity. In ARCFRESH, we will explore extending this method to other straits (e.g., Fram and inbetween Arctic Regions) to validate freshwater flux estimates traditionally based on DOT gradients, leveraging OBP's ability to capture mass-driven flow in sea ice areas.

Knowledge Gaps

Limited Spatial Resolution: GRACE's ~300 km resolution leads to leakage effects, where land mass changes (e.g., Greenland ice sheet melt) contaminate ocean signals. This contamination is acute in the Arctic, where land mass variations dwarf ocean changes per unit area. Filtering techniques using *a priori* land mass models (Wiese et al., 2016) mitigate this, but OBP near ice caps remains unreliable, with errors up to ~5 cm equivalent water height.

GRACE-gap: A 13-month GRACE-GAP (June 2017–July 2018) between GRACE and GRACE-FO disrupted long-term records. Efforts to bridge this with in-situ OBP or altimetry (Peralta-Ferriz et al., 2016) were hampered by sparse coverage, underscoring the need for uninterrupted satellite data.

Validation Scarcity: In-situ OBP gauges (e.g., BPRs in Fram Strait) validate GRACE locally (Morison et al., 2007; Peralta-Ferriz et al., 2014), but their scarcity—especially over the Siberian Shelf or central Arctic—limits basin-wide accuracy. Discrepancies can reach ~2–3 cm equivalent water height (EWH) due to undersampling.

Glacial Isostatic Adjustment (GIA): GIA is poorly constrained in the Arctic, introducing OBP uncertainties of ~2–5 cm EWH (Wake et al., 2016). This affects mass budget closure and FWC estimates.

3.2.3 Sea surface salinity

State-of-the-art

The Sea Surface Salinity (SSS) is a critical indicator of the freshwater flux at the surface of the Arctic Ocean. The meteoric freshwater flux, river discharge, melting and freezing ice have a signature at the ocean surface, diluting and concentrating the SSS. The SSS also play a fundamental dynamical role in the Arctic Ocean, since in cold water, it is the main driver of the density and oceanic currents, and is linked to the upper ocean stratification variability (Carmack et al., 2016). This has a major impact for redistributing heat and freshwater, but also biogeochemical tracers and ecological species, horizontally and vertically between the deeper oceanic layer and the surface. However, this variable remains poorly constrained and modelled in the Arctic Ocean (Carmack et al., 2016).

In various regions of the Arctic Ocean, the SSS has been shown to be a relevant proxy for ocean FW content. For instance, using a model, Fournier et al. (2020) have shown that the SSS variability is significantly correlated with those of SSH-minus-OBP in the Arctic basin, except within the Beaufort Gyre and the regions affected by the subpolar North Atlantic inflow. This relationship has allowed us to better understand the recent redistribution of freshwater over the Siberian shelves and Beaufort gyre (Hall et al., 2022, 2023).

However, during the melting season, this relationship can be obscured by the presence of meltwater thin layers (typically a few metres depth) that result in a large near surface salinity dominated stratification (Peralta-Ferriz et al., 2015). In contrast, these strong SSS anomalies can be related to intense FW flux from sea ice melt. Indeed, satellite observations have previously revealed that sea ice melt can result in localized strong salinity anomalies (up to 5 pss) that can survive over a few weeks (Supply et al. 2022, De Andres et al., 2024, van Straaten et al., 2025), but the processes determining how the melt impacts the ocean surface properties (salinity, temperature, currents) are not fully understood yet.

The Arctic river discharges have also a strong signature in the regional SSS that are linked to the variability of the FW rivers flux, the oceanic and atmospheric forcing on the freshwater plumes. Given the strong signal-to-noise ratio of the satellite measurements in river plumes region, they have been monitored for the first time from intra-seasonal to interannual scales (Matsuoka et al. 2016; Tarasenko et al., 2021). However, further work is needed to fully understand the river plume interaction with ocean, atmosphere, and sea ice dynamics in the Arctic, and the contribution of the river FW input in the regional Arctic FW budget (Hudson et al., 2024).

Since 2010, L-Band radiometer satellite missions, including SMOS (2010-present; Font et al., 2010), Aquarius (2011-2015, Lagerloef et al., 2008) and SMAP (2015-present, Piepmeier et al. 2017) have provided SSS measurements at global scale with a spatial resolution between 100 km and 45 km. This has unprecedentedly stimulated research on SSS variability and led to a more comprehensive understanding of ocean global fresh water cycle (e.g. Boutin et al., 2023a). Yet, at high latitude, L-Band radiometers are recognized to be less sensitive in cold water (Boutin et al.,2023b}, and sea ice contamination is still a serious concern to retrieve SSS in the vicinity of the sea ice edge. Recent advances in L-Band satellite data retrieval and processing, in sea ice filtering and the synergy between L-Band satellites (SMOS, SMAP, Aquarius) and in situ measurements (Tang et al., 2018 ; Olmedo et al., 2018; Supply et al., 2020 ; Kolodziejczyk et al., 2021 ; Martinez et al., 2022) have resulted in improving the signal-to-noise ratio in cold water allowing potential future advances of our understanding of the SSS variability and ocean dynamics in the Arctic demonstrating the capability of L-Band at high latitudes.

In this project, we will build on the most recent climate time-series of SSS from space developed and delivered in the framework of the ESA CCI+SSS project (Boutin et al., 2021). Within the second phase of the CCI+SSS project, the CCI+SSS “Arctic Option” has focused on the improvement of Arctic products, delivering a merged SMOS/SMAP/Aquarius SSS products with the best quality in the Arctic regions. These advances have also improved the consistency of the SMOS-only Arctic product (longest time series: 14 years) delivered at the SMOS CATDS CEC (see relevant ECV dataset below).

Knowledge gaps

Knowledge gaps for SSS in the Arctic relate to gaps in the understanding on how ice melt, P-E, and river discharge influence SSS at different scales. One major gap is detecting and quantifying the freshwater flux signatures from these sources in SSS data, which vary from large to regional scales (e.g. Van Straaten et al., 2025). Additionally, accurately linking SSS variations to overall FW content within the Arctic's complex and dynamic environment remains challenging. These gaps underscore the need for advanced observational techniques and models to better capture the intricate processes affecting Arctic SSS.

3.3 Freshwater source and sink

3.3.1 Land Ice

State-of-the-art

The Greenland Ice Sheet (GIS) and other glaciers and ice caps in the Arctic are losing mass at accelerated rates thereby representing a positive FW Fluxes (FWF) in the Arctic Ocean (e.g. The GlaMBIE Team, 2025; Otosaka et al., 2023; Sommer et al., 2022; Hugonnet et al., 2021; King et al., 2020; Zheng et al., 2018; Box et al., 2018; Enderlin et al., 2014; Gardner et al., 2013). The meltwater runoff from Arctic glaciers and ice caps (including the ice sheet))has been estimated to 473±77 km^3/yr (15.0 ± 2.4 mSv) of freshwater in the period 1961–1992, with an increase to 690±134 km^3/yr (21.9 ± 4.3 mSv) in the period 1993–2006 (Dyurgerov et al., 2010). This freshwater flux plays a crucial role in various Arctic processes, including ocean and fjord circulation patterns, marine ecosystems, and climate dynamics. The exact contribution of land ice to the Arctic FWF can vary depending on factors such as ice discharge and rate of surface melt as well as regional climate conditions and changes in precipitation patterns. However, as global temperatures rise due to climate change, there has been an observed increase in calving and melting of Arctic land ice that is expected to continue in the future, leading to a larger freshwater input into Arctic waters. The FWF contribution from land ice includes three major processes:

1. Solid ice discharge (calving from marine terminating glaciers)
2. Surface runoff (surface melt minus retained water by refreezing and local storage)
3. Basal runoff (melting and discharge from the base of the ice sheet/glacier)

The contribution from these processes can be estimated using satellite-derived ice velocity and elevation change in combination with models (climate, geothermal, ice sheet) as well as ice thickness information.

The solid ice discharge (or Mass Flux and Ice Discharge - MFID), is estimated at predefined gates which are located in general near the grounding line or calving front of marine-terminating outlet glaciers (e.g. Mankoff et al., 2020; King et al., 2018; Enderlin et al., 2014). To calculate the calving flux the depth integrated ice velocity and ice thickness at the gate are needed. Year-round continuous ice velocity data can be derived from repeat pass SAR satellite data (e.g.. Copernicus Sentinel-1), while ice thickness information is available from models, such as IceBridge BedMachine for Greenland (Morlighem et al., 2017), that are generated from data collected by airborne and ground-based radar sounders and bathymetry data in combination with the principle of mass conservation. For MFID this project builds on the achievements of the Greenland Ice Sheet and Glaciers CCI and CCI+ projects since 2012, and on work performed within the ESA STSE Arctic + project ArcFlux. The major advancements emerging from these projects are the development and implementation of an automatic system for the generation of ice velocity (IV) maps from repeat pass Copernicus Sentinel-1 (S1) SAR data by project partner ENVEO (Nagler et al., 2015), and the production of a time-series of ice velocity for the Greenland Ice Sheet margins and several other Arctic ice caps, taking full advantage of the systematic acquisition planning of S1 (2014-present). The monthly and annually averaged IV maps and unprecedentedly dense IV time series of outlet glaciers provide essential information for studying temporal fluctuations and long-term trends and provide key input for ice dynamics, climate modelling and for the calculation of MFID. Within Greenland Ice Sheet CCI+, MFID was added as a new ECV and the IV system was further extended with an MFID module for routine ice discharge calculation based on the IV data from Sentinel-1. This system calculates the solid ice discharge for more than 250 fast flowing outlet glaciers around Greenland representing the majority of the ice discharge.

The surface runoff from the ice sheet has increased significantly over the last 20 years (Trusel et al., 2018), and models project the amount of runoff will continue to increase into the future (Lenaerts et al, 2015). A recent study by Fettweis et al. (2020) intercompares Surface Mass Balance (SMB) components over Greenland from 13 state-of-the-art climate models and shows that there is currently a large variability in the predicted runoff based on model runs. Current state-of-the-art studies are based on models alone (e.g. Bamber et al., (2012), van den Broeke et al., (2016)).

The last contributor, the basal runoff, has until recently been neglected in hydrological assessments of the Greenland Ice Sheet. Karlsson et al., 2021 showed that this contribution can be regionally important. The basal melt is generated by geothermal heat, from friction and from the viscous heat from surface-to-bed transport of melt water, and such a dataset has been generated at drainage basin scale (Karlsson et al., 2023).

In the ongoing ESA POLAR+ project 4DGreenland, a method has been developed to maximize the use of EO data to determine total monthly runoff. This method relies on many different EO data but also models to estimate each component of the ice sheets hydrological components. Currently runoff time series for five different drainage basins have been generated within the project, but it is expected that the analysis will be carried out on an ice sheet scale in the near future.

Within the ESA project ArcFlux — a precursor of this project — a system was tested to generate and combine MFID data, based on ESA CCI ice velocity maps, and modelled runoff estimates from an ensemble of regional climate models (RCMs) to compute the annual freshwater flux contribution from northern Greenland drainage basins for the period 2015-2019 in order to improve estimates of the total Arctic FWF (Andersen et al., 2019). The work performed in this project will fully benefit from the algorithm developments from these projects by exploiting the existing archive and innovative methods.

Gain of accuracy and knowledge

Within the ArcFlux and Greenland CCI+ projects several knowledge and data gaps were identified that were recommended to be addressed for a forthcoming full assessment of the land ice contribution to the Arctic FWF. Closing or narrowing down these gaps is proposed as an optional activity in Option 2 (provided as Annex of the ARCFRESH project proposal).

Ice discharge estimates have so far only been provided for Greenland based on ice velocity at 250 m resolution on an annual scale. This leaves large uncertainties regarding contributions from other regions (e.g Svalbard, Canadian and Russian Arctic), short-term fluctuations (e.g. monthly, seasonally) and the contribution of the many smaller glaciers that are not well resolved on a 250 m grid. A more accurate and complete Arctic assessment therefore necessitates a consistent, spatially and temporally dense, pan-Arctic ice velocity product, processed in a homogenised manner, and at a finer temporal (e.g. monthly) and spatial scale.

Ice thickness at the grounding line is an essential input for determining glacier discharge. However, outside of Greenland, there is very limited information on ice thickness. Even for Greenland ice thickness data is scarce in some regions or relatively far from the grounding line requiring sophisticated interpolation schemes to fill in data gaps. In addition, due to surface wasting, ice thickness models require corrections for elevation change, but this data is currently only available for the Greenland Ice Sheet and not for other ice caps in the Arctic. At present this lack of suitable ice thickness information for many tidewater glaciers forms a major restraint for a complete Arctic inventory of solid ice discharge. However, estimates of the cross sectional areas of calving glaciers can also be made based on measurements of the lengths of ice cliffs/calving fronts and assumptions about the thickness of glaciers in contact with sea water based on extrapolated data from radio echo sounding or glacier freeboard/cliff heights derived from satellite or airborne altimetry (Blaszczyk et al., 2009; Wuite et al., 2015).

As mentioned already, there is a large variability in the ice sheet surface runoff predicted from regional climate models, and a clear knowledge gap is that this parameter at present cannot be measured from space. Therefore, RCMs are essential, and currently the state-of-the-art CARRA reanalysis domains (Nielsen et al., 2022) does not cover the entire Arctic Ocean, and furthermore does not include a surface mass balance model to quantify runoff. CARRA-2 is foreseen to be released within the timeframe of this project and will cover the whole domain. An additional knowledge gap is the basal melt under other/smaller ice caps than the main Greenland ice sheet (Karlsson et al., 2023).

In this project estimates of solid ice discharge, surface runoff and basal melt are combined to estimate the contribution of the FWF from Land Ice to the Arctic Ocean and generate time series of this quantity at high spatial and temporal resolution. An explorative study to achieve this was done in the project ArcFlux where a snapshot in time of the FWF was calculated for several basins. The FWF estimates calculated within this project have much potential to enhance the state-of-the-art in various aspects. In particular, the estimates will be based on the latest available ice velocity, ice thickness and model data sets, the spatial and temporal sampling is unprecedented, and also include methodological improvements. The overall work performed in this project will help pave the way to a more systematic approach for FWF quantification from Land Ice, allowing for an unprecedented detailed regional appraisal of FWF mapping in the Arctic Ocean and enabling to assess long term trends and interannual variability.

3.3.2 Sea ice

State-of-the-art

Sea ice FWF are typically estimated through sea ice volume fluxes, which combine measurements of sea ice thickness, concentration, and drift across the Arctic Ocean (e.g., Vinje, T., 2001, Spreen et al., 2020; Moore et al., 2021; Sumata et al., 2022; Howell et al., 2024). Typically, sea ice fluxes in the Arctic are evaluated at specific ocean gates (Fig. 5). The Arctic Ocean is surrounded by land masses that form a natural boundary for moving sea ice in the Arctic. At the same time, there are gates to the sub-Arctic Seas, through which sea ice is exported (Fig. 5). The main export gates are the Fram Strait and Davis Strait, where sea ice is transported southward into the North Atlantic. Notably, the Fram Strait alone accounts for approximately 25% of the total freshwater export to the North Atlantic (Lique et al., 2009). Changes in export through this strait have the potential to influence global thermohaline circulation by affecting deep water formation in the North Atlantic (Dickson et al., 1988). Sea ice volume export through the Fram Strait is also a key contributor to Arctic sea ice mass balance, with variability primarily driven by ice drift linked to large-scale atmospheric circulation, and accounting for half of the interannual changes in Arctic winter multi-year ice volume (Ricker et al., 2021). Moreover, the variability in the Arctic sea ice export contributes significantly to the variations in surface salinity in the subpolar gyre, and in particular in the regions where deep convection occurs, such as the Labrador and Greenland seas (Selyuzhenkok et al., 2020).

Estimating sea ice volume fluxes requires the multiplication of sea ice motion, thickness, and concentration. Those products are provided on different time and spatial scales. Ricker et al. (2018, 2021) have used monthly sea ice thickness gridded products in combination with daily grids of sea ice concentration and drift. These are reprojected and interpolated on monthly 25 km Equal-Area Scalable Earth (EASE-2) grids. Then, ice volume flux is computed from gridded ice drift, concentration, and thickness, and is integrated over the considered flux gates, distributed across the Arctic.

Uncertainties in volume fluxes primarily depend on the uncertainties of the underlying ice thickness, concentration and drift products. These are currently assessed using a 'Gaussian error propagation approach' (which is similar to, but may not be identical to the GUM law of propagation of uncertainties). For example, per 25 km grid cell, ice volume flux uncertainty is typically around 0.1 $km^3\ day^{-1}$ (e.g., Ricker et al., 2018). In the Fram Strait, an array of upward looking sonars can be used to retrieve sea ice thickness and compute volume fluxes (Vinje, T., 2001, Spreen et al., 2020, Sumata et al., 2022) for validation of the satellite estimates. But to retrieve spatially distributed FWF estimates, we primarily rely on satellite measurements. For sea ice thickness, most of the studies have used altimetric products such as from CryoSat-2 (Ricker et. al, 2018; Landy et al., 2022). To map the area flux, many studies use sea ice concentration and drift data from passive microwave products (e.g., Krumpen et al., 2016). However, especially in regions with high drift rates such as Fram Strait, passive microwave ice drift products exhibit significant uncertainties in the range of 1.0 $km\ day^{-1}$ (Sumata et al., 2015). In contrast, ice drift derived from high resolution synthetic aperture radar (SAR) imagery (e.g., RADARSAT-1/2,Sentinel-1, and the RADARSAT Constellation Mission (RCM) provide more representative drift speed estimates compared to lower resolution passive microwave estimates (Kwok et al., 1998; Moore et al., 2021; Howell et al., 2024). However, SAR imagery has limited temporal coverage until 2016 when RCM and Sentinel-1 can be combined to increase temporal resolution(Howell et al., 2022).

Within the previous ESA ArcFlux project, the ice volume fluxes and associated freshwater fluxes were estimated in the Fram Strait for October 2014-April 2015 to prove the concept of combining monthly CryoSat-2 derived sea ice thickness products, daily OSI-SAF sea ice concentration maps with SAR-derived drift vectors. The stated uncertainties of the different CryoSat-2 sea ice thickness products were found to be substantially larger than inter-product discrepancies. Related uncertainties by using existing snow depth estimates (Warren et al. 1999, Forsström et al. 2011) and ice densities (using either only first-year ice (FYI) or multi-year ice (MYI) densities by Alexandrov et al. 2010) were estimated to be 2%-7% and 6% of the total sea ice FWF (Andersen et al., 2019). At the time of the ArcFlux project there were no other studies within the same time period, but the estimated sea ice volume fluxes of similar magnitude as the study by Spreen et al. (2009).

Knowledge gaps and expected gain

To date, scientific studies have mostly concentrated on Fram Strait, considering different types of sensors and over different periods. However, flux estimates from across the Arctic using satellite remote sensing covering the early 2000s require consistent data records across subsequent satellite missions (e.g., Envisat (2002-2012), CryoSat-2 (2011-)). Therefore, the proposed work will benefit from the CCI data records. Moreover, uncertainty estimation so far has largely assumed measurement errors are uncorrelated spatially and temporally. This approach will be revised in the proposed project. A source of uncertainty comes from the snow on sea ice, where we currently use a snow climatology for the computation of the CCI sea ice thickness records. It utilizes a merged snow product over first-year sea ice that is based on the monthly Warren snow climatology (W99) together with daily snow depth from AMSR2 data, provided by the Institute for Environmental Physics of the University Bremen. Snow depth over multi-year sea ice is solely based on the W99 snow depth (Paul et al., 2024). Using an improved snow depth representation that also reflects interannual variability would likely decrease the uncertainty estimates in FWF as found in Andersen et al. (2019). However, exploiting alternative snow depth products to derive sea ice thickness have already been addressed in the CCI+ project.

The altimetry-based sea ice thickness products leave a significant gap around the poles (CryoSat-2: >88°N, Envisat: >81.4°N). To retrieve a complete pan-Arctic FW budget, we need to interpolate at the pole holes. This is also addressed in the CCI+ project, but it remains unclear whether a timely solution is available for this project. However, considering ocean gates that are located at or below 81.4°N will mitigate this challenge.

Sea ice drift from passive microwave radiometry is typically underestimated in regions with high drift rates, e.g. Fram Strait (Sumata et al., 2015). Therefore, we will also make use of ice drift derived from SAR to better quantify the uncertainties and compute reference volume fluxes over a limited period of time.

Estimates of sea ice volume fluxes often neglect snow, which is transported along with the sea ice, covering its surface. The CCI sea ice thickness product contains a snow depth/density climatology, but therefore any interannual variability is neglected. We will quantify the uncertainty in the computation of FWF that results from using climatological snow depth estimates, using findings from snow depth intercomparison studies (Zhou et al., 2021).

Due to the presence of melt ponds, retrieving sea ice thickness from altimetry during summer (May-September) is challenging (Laxon et al., 2013). Landy et al. (2022) recently developed a year-round ice thickness product for the CryoSat 2 period (2011-2020), which has the potential to bridge the gap in summer. However, the method is not applicable to previous satellite missions (e.g., Envisat, ERS1/2). The reason is that Envisat and ERS1/2 are pulse-limited altimeters with large footprints and generally coarser resolution. This makes it difficult to apply the method to retrieve summer freeboard and thickness.

3.3.3 Riverine Discharge

State-of-the-art

The available in-situ observations of river discharge represent only approximately 60% of the pan-arctic river drainage basin (PADB) draining into the Arctic Ocean. Despite this large gap in the monitoring network, different estimates of the total river flux to the Arctic Ocean based on the in-situ observations are relatively consistent as summarised by Shiklomanhov et al (2021); the long term average annual flow is about 200-226 mm/year depending on the investigated domain and extrapolation methods, corresponding to a total flux to the ocean at about 4300 km^3 per year (~136 mSv, milli-sverdrup); the distribution in space shows that about 55% comes from rivers in Asia, 28% from North America, and 17% from Europe; the long-term records show a significant increase in river discharge over time (the total river flow to the ocean increased with 210 km^3 over 1936-2015 from Eurasia, and 64 km^3 from North America over 1964-2015). These increases in the annual river flux mainly result from an increase in the winter and spring flows, and could be coupled to increasing summer-fall and wintertime precipitation, thawing permafrost, and earlier onset of snowmelt and river ice breakup (eg. Shiklomanov et al, 2021; Stadnyk et al, 2021; Lebedeva and Gustafsson, 2021; Hiyama et al, 2023). In addition to the climate change related changes in the river flow, increased use of Arctic rivers for hydropower production and other human regulations contributes to changes in the seasonality, typically expressed as a general flattening of the annual distribution, with a earlier but lower spring flood peak, increases in the low flows during winter and autumn but less significant changes in the summer. As pointed out by Shiklomanov et al (2021), the impact of human regulations largely affect the river discharge in several of the large Arctic rivers such as Yenisei, Lena and Ob, and cannot be neglected when analysing the climate change impacts on the river flow to the Arctic Ocean.

Knowledge gaps and expected gain

The WMO Arctic-HYCOS project, including the national hydrological services of the Arctic Council member states, has together identified and committed to sustain and make available data from a list of some 420 stations representing river basins of more than 5000 km^2 in size and time series length of more than 30 years. 73 of these stations are so-called flow to ocean stations, being the most downstream station in its river basin. The data from most countries outside Russia is available in real time, whereas data from the Russian stations are available only after 2 years, at best.

As previously stated, the stations in the Arctic-HYCOS station network represent about 60% of the PADB that covers a vast land area of catchment of 23 million km^2 with upstream areas covering several climatic zones reaching as far south as 45 °N.

The ESA CCI River discharge data set, including data from the Lena, Ob, Mackensie and Colville Rivers, represent about 7.3 million km^2. The EO monitoring over Lena and Ob will be highly useful as a complement to the in-situ data, due to the long latency time from the Russian rivers. It should be acknowledged that ESA CCI river discharge is a proof-of concept project that provides data from about 30% of the PADB, most of which is already represented by the in-situ data.

Thus, despite the potential of EO based discharge data to improve the capacity for river discharge observations in the Arctic, there is a need to use hydrological models to interpolate and extrapolate the observations in space and time, in order to provide a consistent ECV record for the river freshwater inflow to the Arctic Ocean. Assimilation of satellite based snow data, as well as river discharge data, has been shown to be useful in improving hydrological model analysis of river discharge, especially in high latitude river basins where water stored in snow, lakes and soil storages provide large controls and memory in the hydrological system (Musuuza et al, 2021, 2023). The Arctic-HYPE model has been developed by SMHI in collaboration with researchers in Canada, Finland, Sweden, and Russia with the aim to provide a consistent pan-arctic hydrological model analysis (Stadnyk et al, 2021; MacDonald et al, 2018; Gelfan et al, 2017, Andersson et al, 2015). However, as with all models, the Arctic-HYPE model is also sensitive to the quality of the meteorological forcing data (temperature, precipitation) and in particular for the Arctic climate, the partition of precipitation into snow and rain. The sensitivity of river discharge predictions to the Arctic Ocean, to the meteorological forcing data, especially concerning the seasonality, was further emphasized by Winkelbauer et al (2022), who published a diagnostic analysis of river flow to the Arctic Ocean using the ECMWF land-surface scheme coupled to a river routing model forced different forcing data sets.

3.3.4 Precipitation-Evaporation

State-of-the-art

The difference between precipitation (P) and evaporation (E), i.e. net precipitation (P-E), is the freshwater flux from the atmosphere to the surface. Methods to derive global P, E and P-E are typically based on satellite or reanalysis data or a combination of both, due to the lack of sufficient in-situ measurements e.g. over the ocean. A recent study by Gutenstein et al. (2021) has compared freshwater fluxes from six satellite-based retrieval algorithms and the ERA5 reanalysis (Hersbach et al., 2020) over the ocean for the period 1997-2013. They find regionally substantial differences among the satellite datasets and to the ERA5 reanalysis. The differences in P-E are generally dominated by differences in precipitation.

Comparing precipitation data from GPCP (Global Precipitation Climatology Project), based on a combination of rain gauges and satellite data (Huffman et al., 2001) to the satellite based HOAPS (Hamburg Ocean Atmosphere Parameters and Fluxes from Satellite Data) 4.0 data (Andersson et al., 2017), and the model based ERA5 reanalyses, Gutenstein et al. (2021) found that at latitudes higher than 50°, the temporal correlations between HOAPS and GPCP, as well as ERA5 and GPCP are small, indicating particularly large differences between the datasets in this region. Over the Arctic Ocean, large P values from HOAPS and ERA5 are lower than in GPCP and low P values are larger than in GPCP, i.e. the precipitation distributions from HOAPS 4.0 and ERA5 are more centred than from GPCP. However, at latitudes between 40° and 70°, GPCP is also known to have a high bias (Andersson et al., 2017) and the differences should be handled cautiously.

The analysis by Gutenstein et al. (2021) further shows that satellite-based estimates of E and P are less consistent with each other (as they are measured from different satellite missions) than E and P derived from ERA5 (outputs provided by the same reanalysis). Such consistency is an important prerequisite to close the FWF cycle. ERA5 has also been shown to outperform other reanalyses in the Arctic due to its high spatial resolution and data assimilation techniques (Barrett et al., 2020) and estimates of P-E in the Arctic based on ERA5 agree well with prior estimates (Ford and Frauenfeld, 2022). On the other hand, ERA5 underestimates seasonal and interannual variability of P-E compared to satellite-based data (Gutenstein et al., 2021). Here, locally tailored and even higher resolved regional reanalyses, like the Copernicus Arctic Regional Reanalysis (CARRA), can potentially provide an added value.

Knowledge gaps

There are significant differences between the available datasets of E, P and P-E in the Arctic. The differences in P-E are mostly governed by differences in P. However, in-situ measurements of P in the Arctic are particularly difficult due to low temperatures and high winds, resulting in a low number of, mainly land-based, stations. Thus, the P-E FWF over the Arctic Ocean remains uncertain.

3.3.5 Ocean gateways

State-of-the-art

The primary ocean flux gates—Bering Strait, Davis Strait, Fram Strait, and the Barents Sea Opening (see Figure 1a)—are the largest pathways for freshwater flux into and out of the Arctic Ocean. Traditionally, in-situ measurements at these sites provide freshwater flux (FWF) estimates (Woodgate & Aagaard, 2005). Pacific water enters via the Bering Strait, significantly modifying Arctic water mass characteristics and contributing up to 40% of the Arctic's freshwater budget, as Pacific water are relatively fresher than the water of the halocline (Woodgate & Aagaard, 2005). This inflow influences the freshwater content in the Arctic and via its outflow through the Fram strait indirectly the stability of the Atlantic Meridional Overturning Circulation (AMOC) and exhibits notable interannual variability, peaking in 2004 (Woodgate et al., 2018).

The ESA ArcFlux project (Andersen et al., 2019) demonstrated that Dynamic Ocean Topography (DOT)—derived from satellite altimetry by subtracting the geoid from sea surface height (SSH)—can map mean surface slopes, geostrophic currents, and seasonal water transport variations across these gates. To estimate the freshwater fluxes from the total water transport, we need knowledge about the salinity. Depth-integrated freshwater transport (FWT) across a defined gate is calculated as:

$$FWT(x,z) = \int_{X_2}^{X_1}\int_{0}^{Z} -\frac{g}{f}\frac{\partial DOT}{\partial x}\left(\frac{S_{ref} - S(x,z)}{S_{ref}}\right)dxdz \tag{7}$$

where g is gravitational acceleration, f is the Coriolis parameter, S(x,z) is salinity at position x and depth z, and Sref=34.8 pss is the reference salinity (Solomon et al., 2021).

The ESA ArcFlux project combined satellite-observed sea level with in-situ mooring data, demonstrating that freshwater flux (FWF) through Bering Strait aligns with literature estimates from Woodgate et al. (2018) (~2500–3000 km³/yr, 2001–2014),), driven by rising volume transport (~1.1 Sv or ~35,000 km³/yr by 2014) and a fresher Pacific inflow. This is though with reduced accuracy compared to in-situ methods (Andersen et al., 2019).

To reduce uncertainties in FWF contributions to the Arctic FW budget, all pathways—including smaller straits like Hekla Strait in the Canadian Arctic Archipelago, connecting to Hudson Bay and the Atlantic—must be assessed. Current limitations include sea ice contamination of conventional altimetry observations (e.g., Jason-3, Sentinel-6 MF, Envisat), which introduces uncertainties of ~10–15 cm in sea level, translating to FWF uncertainties of ~500–1000 km³/yr across gates like Bering Strait (Andersen et al., 2019). CryoSat-2's SAR mode reduces this to ~5 cm (Rose et al., 2019), which lowers FWF uncertainty to ~200–500 km³/yr. Additional challenges stem from determining salinity profiles, with mooring-based salinity errors of ~0.1–0.2 psu contributing ~100–300 km³/yr uncertainty in FWF estimates (Woodgate et al., 2018). The uncertainty associated if sea surface salinity observations are used as a proxy, is still to be determined, but will likely increase the FWF uncertainty significantly compared to if in-depth salinity from in-situ observations is used for estimating FWF.

Knowledge gaps

Gridded data for flux estimation. No studies have yet demonstrated that gridded and interpolated CCI Sea Level data can reliably determine FWF through Arctic Ocean flux gates (e.g., Bering, Davis, Fram Straits). While Peralta-Ferriz and Woodgate (2023) successfully used gridded Dynamic Ocean Topography (DOT) from satellite altimetry and GRACE data (2013–2014) to estimate Bering Strait FWF (~3500 km³/yr), they noted that older gridded and interpolated satellite datasets (pre-2011) lacked sufficient quality for such analyses due to coarse resolution and ice-related errors. Along-track, high-resolution DOT products offer superior sea level accuracy, potentially matching in-situ flux gate estimates (Andersen et al., 2019), but these are not yet widely available for Arctic flux gates.

Geoid accuracy. DOT accuracy remains constrained by limited geoid knowledge in the Arctic, with uncertainties of ~2–5 cm in the Arctic (~200-500 FWF km³/yr).

Salinity data. In the ARCFRESH project we will use in-situ data for estimating in-depth salinity, but these observations are limited both in time and space. Bering, Fram and Davies straits are well covered with moorings, but in other areas satellite sea surface salinity observations or reanalysis models will be utilized as a proxy for in-depth salinity.

4 Uncertainty approaches and considerations

One of the key themes of the ARCFRESH project is to bring a metrological perspective to how the project handles observational and modelling uncertainties, in order to ensure the robustness and credibility of the derived estimates and budget closure. A systematic approach to quantifying these uncertainties allows for improved interpretation of observational data, enhances model validation efforts and ultimately supports more reliable assessments of freshwater contributions to Arctic climatic and oceanographic processes. While the metrological approach provides a valuable framework for characterising uncertainties, its practical application is constrained by the limited availability of comprehensive uncertainty information, particularly in complex and data-sparse environments. Consequently, this project also presents an opportunity to explore innovative methodologies for integrating measurement and modelling uncertainties, and as a test-bed for broader research efforts that combine multiple different observational datasets with modelling efforts.

4.1 What makes a metrological uncertainty approach?

A recent paper (Woolliams et al., 2025) summarises what is involved in 'a metrological approach to uncertainties'. It defines such an approach as following the Guide to the Expression of Uncertainty in Measurement (GUM). The GUM is a suite of documents available at https://www.bipm.org/en/committees/jc/jcgm/publications which includes the original 2008 'legacy GUM' (JCGM100), along with several supplementary documents summarised in (JCGM GUM 1). The metrological approach involves the following aspects (quote from Woolliams et al., 2025):

- Consistent terminology including a clear distinction between 'error' and 'uncertainty',
- Well-defined measurand with an associated measurement model having input quantities and measurand(s) as output quantities,
- Measurement model incorporating in its input quantities all known effects including correction terms relating to known biases.
- Propagation of uncertainties (and covariances) through the same measurement model that is used to calculate the measured value (the estimate of the measurand).

It is clear from this list that the availability of a suitable measurement model is central to a metrological approach. The measurement model describes how the measurand — the quantity intended to be measured — is calculated from input quantities. It is often written by an analytic (algebraic) expression, but measurement models may also be defined through code, particularly where iterative processes and inverse problem solution methods are used, or when there are classification or similar steps in the processing. Note that the measurement model does not necessarily describe a pure 'measurement', indeed it is common for the measurand to be calculated from the input quantities through some appropriate model. In real measurement scenarios, the measurement model is also usually a 'multi-stage measurement model', in that the input quantities to the calculation of the final 'measurand' are themselves calculated from their own measurement models.

Another core aspect of a metrological uncertainty assessment is the clear distinction between 'uncertainty' and 'error'. The International Vocabulary of Metrology (VIM), in its current (third) edition (JCGM 200) defines measurement error as 'measured quantity value minus a reference quantity value' and measurement uncertainty as 'non-negative parameter characterizing the dispersion of the quantity values being attributed to a measurand, based on the information used'. The error is almost always unknown (because if it were known, it would be corrected for, to create a 'measurement model incorporating all known effects'). It is the unknown difference between the measured value and a true value. The standard uncertainty is the standard deviation of the distribution around the measured value in which the true value is expected to lie. In most cases, where the distribution is symmetrical, the uncertainty also describes the distribution of possible errors.

The recent paper (Woolliams et al., 2025), presents the QA4EO Five Steps (also available at www.qa4eo.org), themselves a refinement of the uncertainty approach (Mittaz et al., 2019) developed in the FIDUCEO (https://research.reading.ac.uk/fiduceo/) and GAIA-CLIM (https://www.gaia-clim.eu/) projects. The Five Steps approach is summarised in Figure 4.1. QA4EO is the Quality Assurance framework for Earth Observation and is a set of principles endorsed by the Committee on Earth Observation Satellites (CEOS) and the Global Satellite Intercomparison System (GSICS). The QA4EO approach has also been highlighted in the Global Climate Observing System (GCOS) 2022 Implementation Plan (GCOS, 2022).

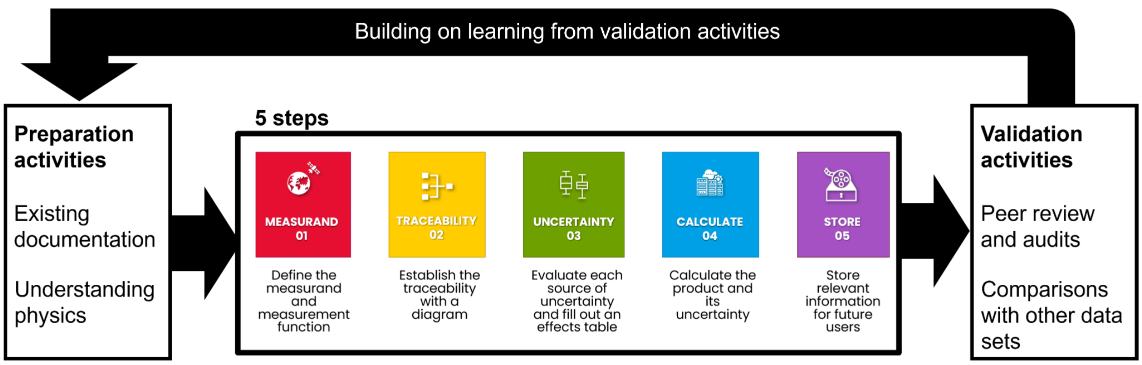

Figure 4.1: The QA4EO Five Steps to uncertainty analysis. Further details are available on (www.qa4eo.org). The Five Steps are given within the central box and are placed within an external iteration loop that represents how such analyses are informed by preparation activities and refined through validation activities.

The Five Steps are as follows:

- Step 1: Define the measurand and measurement model
- Step 2: Establish traceability with a diagram
- Step 3: Evaluate each source of uncertainty and fill out an effects table
- Step 4: Calculate the product and its uncertainty
- Step 5: Store relevant information for future users.

The application of these steps to the ARCFRESH project is discussed further below.

The Five Steps are shown in Figure 4.1 as being within an iterative feedback loop that is informed by validation activities involving both peer review and comparisons across datasets.

4.2 Application to modelled data

The QA4EO Five Steps approach was developed for observational data. Initially it was developed for radiometric satellite observations, and it has since been applied to a wide range of passive and active remote sensing techniques from satellite and non-satellite platforms, as well as to in-situ observational methods. With appropriate interpretation, the Five Steps can be applied to any measurement process or observational dataset. What is less clear is how to apply that approach, or a similar approach, to simulated data that has been created using a model. Models can use observational data to constrain boundary conditions, in data assimilation or for validation purposes. In any of these cases, we must propagate uncertainties associated with the observational data into the modelling process. Beyond that, consideration is needed to assess the uncertainties associated with the models in a metrological way.

We hope that the ARCFRESH project will provide an opportunity to have conversations between metrologists, observational experts and modelling experts to make the first steps towards a consistent metrological approach to modelled data.

4.3 Application of the Five Steps to ARCFRESH observational datasets

The first step in the Five Steps is to define the measurand. This step is far from trivial. In the ARCFRESH project the highest level measurand is the ‘freshwater flux into and out of the Arctic Ocean’. A full definition of the measurand requires clarity around all aspects of this: what is meant by ‘freshwater’, by ‘flux’ and by ‘Arctic Ocean’. In the first project uncertainty workshop, these three aspects were discussed in detail, but are not fully resolved at this stage of the project. ‘Freshwater’ can be interpreted as a volume (at a given temperature) or as a mass of salt-free water in liquid state. Such a definition would have to include an analysis of how to convert a sea ice volume into a fresh water volume. Alternatively, analysis could be based on salinity content (see also Section 2.5). Flux implies a change over time through a particular section, meaning it does not address the freshwater content, but its rate of change. By ‘Arctic Ocean’, it is implied that its mass of water is contained within some geographic boundaries, either land masses, oceanic gateways or sea surface and bottom. The project is considering options for defining the outer boundaries of the control volume and the inner ocean subsections (Section 2.6). It is not a metrological task to make these definitions, but it is important from a metrological perspective that these concepts are unambiguously defined, or rather that the uncertainty associated with the definition is included in the uncertainty assessment. In the ARCFRESH project, we will attempt to balance the sum of fluxes from each of the different transport mechanisms with the change in freshwater in the Arctic Ocean calculated directly. This analysis requires that the measurand is the same for all quantities.

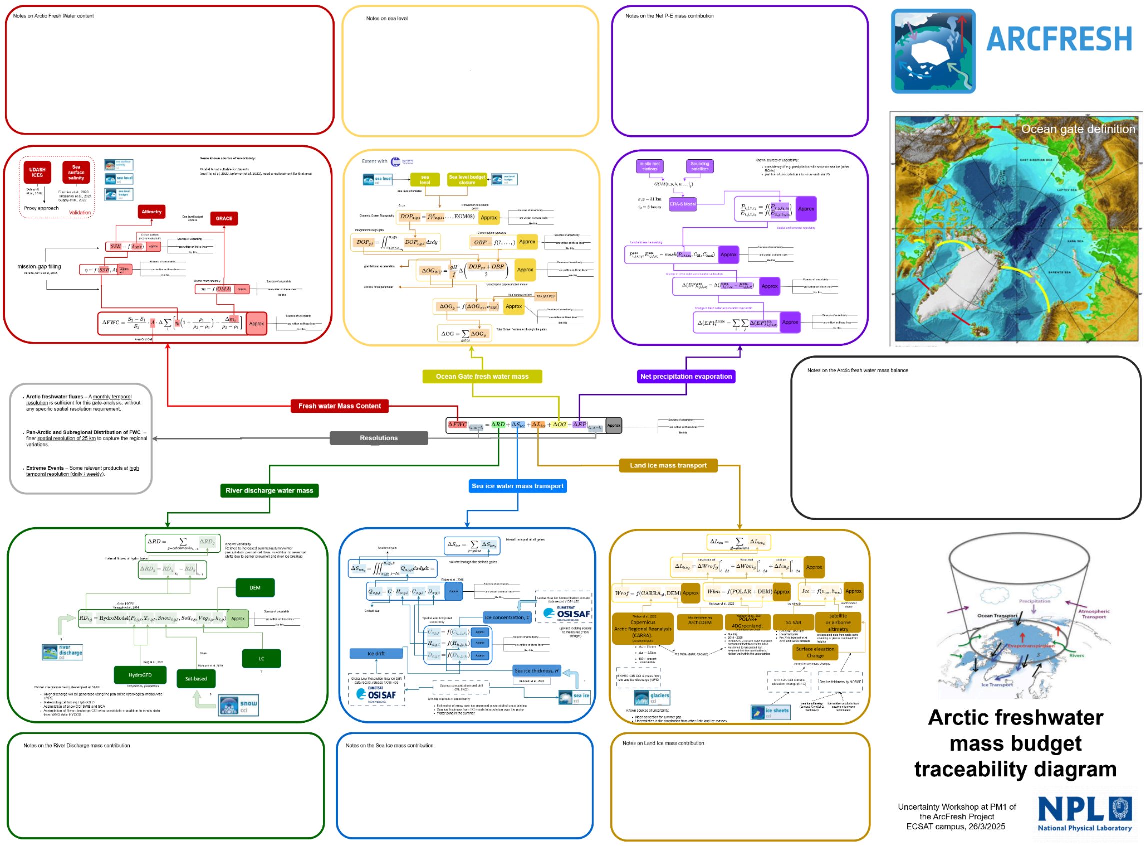

Figure 4.2: Overview of the ARCFRESH project uncertainty tree diagram that was discussed at the workshop. This is available to project partners and ESA in its current state, but is currently being edited, so is left unclear here.

The second step of the Five Steps is to show the traceability with a diagram. Uncertainty tree diagrams, initially developed in FIDUCEO and GAIA-Clim, have been found to be particularly useful to present the multi-stage measurement model in a diagrammatic way and to show how uncertainties associated with input quantities propagate to the measurand of interest. During the uncertainty workshop, the diagram shown in Figure 4.2 was discussed. Note that this is only shown conceptually (details are not visible) because it is a work in progress. The central equation of this diagram describes the main relationship being assessed in this project, namely the relationship between changes in freshwater flux within the Arctic Ocean and the sum of the individual flux components. Each flux component is then described by its own diagram.

The third step of the Five Steps is to assess each source of uncertainty using an effects table, which documents everything that needs to be known about a source of uncertainty: namely, the magnitude of the uncertainty, and its error correlation structures in spatial and temporal dimensions. Such error correlation information is necessary to propagate uncertainties appropriately through regridding, integration and averaging — processes that are essential to assess total fluxes through gates. Most datasets that are being used in the ARCFRESH project come from ESA-CCI datasets. All ESA-CCI projects have provided some form of uncertainty assessment, and most of those include some breakdown of uncertainties into the constituent parts. It is, however, rare for them to include spatial and temporal error correlations (with the possible exceptions of the sea surface temperature and sea level anomaly datasets). A full analysis of uncertainties of the ESA-CCI datasets is beyond the scope of the project, but NPL will review the available information and help the teams make reasonable assumptions about suitable error correlation structures.

The fourth step of the Five Steps is the calculations. In this case that includes assessing freshwater fluxes through both a direct measurement of changes within the Arctic Ocean and through the sum of individual fluxes. Software needs to be developed to propagate uncertainties. Given the limited information about error correlation structures, which are nevertheless important, the software needs to be able to handle both situations where there is sufficient error correlation information and where such information is lacking. The NPL-written CoMet toolkit (https://www.comet-toolkit.org/) can be used as the basis for such a software package. The software will have to handle regridding of datasets: for example to bring sea ice thickness and sea ice velocity data onto the same grid, as well as to integrate over a gate.

The fifth step in the Five Steps is to store information about uncertainties in a way that can be useful to today’s data users and to those who in the future may wish to reanalyse the dataset. Within this project, the direct users of the dataset will be the modellers, and therefore within this step it is necessary to assess how we will provide useful information from observational datasets for modellers. One approach may be to develop an ensemble of observational data with a distribution that describes the uncertainties. Another would be to propagate uncertainty (and error covariance) information into the model. Further work is needed to assess the benefits of each of these approaches. In terms of long-term data preservation, it will be important to provide detailed summaries about the assumptions made in the uncertainty analysis in a way that ensures the datasets are reproducible by future scientists. This will come from high quality reporting, and from the open provision of software used in the project, as well as through well-written scientific papers.

Outside the Five Steps, the iterative feedback process requires an approach to validation. This project, in closing a 'budget' between the changing freshwater in the Arctic and the sum of the individual fluxes builds in its own validation. Furthermore, the comparison of such analysis with the modelling work within the project will further validate the data. Traditionally such approaches were aimed at validating the data: assessing the differences between observations and models to obtain an estimate of uncertainties from the statistical distribution of such differences. However, if we have performed a meaningful uncertainty assessment of the individual contributions, we can calculated the normalised 'E_N ratio', that is, we can calculate:

$$E_N = \frac{A - B - \Delta}{\sqrt{u_A^2 + u_B^2 + u_\Delta^2}} \quad (8)$$

for each comparison, where A and B are the values from the two comparing datasets, with associated uncertainty u_A, u_B, respectively, and Δ is the expected difference between them (e.g., to account for known differences in the measurand), with an associated uncertainty u_Δ. The distribution of such E_N ratio values for multiple comparisons is expected to have a standard deviation of one if the uncertainties are correctly assessed.

Finally, the iterative feedback process benefits from peer review. The highly collaborative cross-disciplinary nature of the ARCFRESH project will enable such reviews to be done in a very fresh way.

5 Conclusions

The review of recent literature has made emerged some remaining scientific questions to address to better understand the FW change in the Arctic.

- Overall, it is still difficult to close FW budget in the Arctic due to missing terms such as e.g. Greenland and glacier melt, comprehensive riverine discharge estimates, and accurate interannual variable ocean FW flux at the Arctic gateways. Missing accuracy and/or long observation time series for freshwater content and fluxes. The accuracy of FW flux at the gateways is particularly sensitive for the FW and steric sea level closure in the Arctic and represent the main knowledge gap to address.
- The regional budget and exchange of FW inside the Arctic is crucial to better understand the dynamic of the Arctic FW system and its future change. This question maybe coupled with the interannual to decadal variability of the atmospheric and oceanic circulation in the Arctic that remain to be disentangled from long term anthropic variability. These space and timescales need to be better addressed with model and observation, especially to better document and understand the impact of the 2007 regime shift on FW regional and pan-Arctic budget.
- The intra-seasonal and extreme events link with FW variability in the Arctic is still to be documented and understood. As the retreat of sea ice will increase the air-sea interactions. It will favor more momentum and heat transfers that will enhance FW transport over the Arctic basin, and transfer between solid and liquid phase. The synoptic satellite time series can help to better address this process in the context of Arctic FW system changes.

References

Aagaard, K., & Carmack, E. C. (1989). The role of sea ice and other fresh water in the Arctic circulation. Journal of Geophysical Research, 94, 14485–14498. https://doi.org/10.1029/JC094iC10p14485

Ablain, M., Cazenave, A., Larnicol, G., Balmaseda, M., Cipollini, P., Faugère, Y., Fernandes, M. J., Henry, O., Johannessen, J. A., Knudsen, P., Andersen, O., Legeais, J., Meyssignac, B., Picot, N., Roca, M., Rudenko, S., Scharffenberg, M. G., Stammer, D., Timms, G., and Benveniste, J.: Improved sea level record over the satellite altimetry era (1993–2010) from the Climate Change Initiative project, Ocean Sci., 11, 67-82, doi:10.5194/os-11-67-2015, 2015.

Alexandrov, V., Sandven, S., Wahlin, J., & Johannessen, O. M. (2010). The relation between sea ice thickness and freeboard in the Arctic. The Cryosphere, 4, 373–380. https://doi.org/10.5194/tc-4-373-2010

Andersen, O. B., Mertikas, S. P., Pail, R., & others. (2019). Arctic freshwater fluxes from Earth observation data. In S. Mertikas & R. Pail (Eds.), Fiducial Reference Measurements for Altimetry (Vol. 150). Springer, Cham. https://doi.org/10.1007/1345_2019_75

Andersson, A., Graw, K., Schröder, M., Fennig, K., Liman, J., Bakan, S., Hollmann, R., & Klepp, C. (2017). Hamburg Ocean Atmosphere Parameters and Fluxes from Satellite Data – HOAPS 4.0. Satellite Application Facility on Climate Monitoring, Data set. https://doi.org/10.5676/EUM_SAF_CM/HOAPS/V002

Armitage, T. W. K., Bacon, S., Ridout, A. L., Thomas, S. F., Aksenov, Y., & Wingham, D. J. (2016). Arctic sea surface height variability and change from satellite radar altimetry and GRACE, 2003-2014.

Bamber, J., Van Den Broeke, M., Ettema, J., Lenaerts, J., & Rignot, E. (2012). Recent large increases in freshwater fluxes from Greenland into the North Atlantic. Geophysical Research Letters, 39(19). https://doi.org/10.1029/2012GL052552 8)

Barkhordarian, A., Nielsen, D.M., Olonscheck, D. *et al.* Arctic marine heatwaves forced by greenhouse gases and triggered by abrupt sea-ice melt. *Commun Earth Environ* **5**, 57 (2024). https://doi.org/10.1038/s43247-024-01215-y

Barrett, A. P., Stroeve, J. C., & Serreze, M. C. (2020). Arctic Ocean precipitation from atmospheric reanalyses and comparisons with North Pole drifting station records. Journal of Geophysical Research: Oceans, 125(1), e2019JC015415. https://doi.org/10.1029/2019JC015415

Behrendt, A., Sumata, H., Rabe, B., & Schauer, U. (2018). UDASH–unified database for Arctic and Subarctic hydrography. Earth System Science Data, 10(2), 1119-1138. https://doi.org/10.5194/essd-10-1119-2018

Bintanja, R., and F.M. Selten. 2014. Future increases in Arctic precipitation linked to local evaporation and sea ice retreat. Nature 509:479–482, https://doi.org/ 10.1038/nature13259

Blaszczyk, M., Jania, J., & Hagen, J. O. (2009). Tidewater glaciers of Svalbard: Recent changes and estimates of calving fluxes. Polar Research, 30, 85–142.

Boisvert, L. N., Webster, M. A., Petty, A. A., Markus, T., Bromwich, D. H., and Cullather, R. I.: Intercomparison of precipitation estimates over the Arctic Ocean and its peripheral seas from reanalyses, J. Clim., 31, 8441–8462, https://doi.org/10.1175/JCLI-D-18-0125.1, 2018.

Boutin, J., et al. (2021). Satellite-based sea surface salinity designed for ocean and climate studies. Journal of Geophysical Research: Oceans, 126(11), e2021JC017676.

Boutin, J., et al. (2023). New seawater dielectric constant parametrization and application to SMOS retrieved salinity. IEEE Transactions on Geoscience and Remote Sensing, 61, 1–13.

Boutin, J., Yueh, S., Bindlish, R., Chan, S., Entekhabi, D., Kerr, Y., ... Zribi, M. (2023). Soil moisture and sea surface salinity derived from satellite-borne sensors. Surveys in Geophysics, 44(5), 1449–1487.

Box, J. E., Colgan, W. T., Wouters, B., Burgess, D. O., O'Neel, S., Thomson, L. I., & Mernild, S. H. (2018). Global sea-level contribution from Arctic land ice: 1971–2017. Environmental Research Letters, ERL-105795. https://doi.org/10.1088/1748- 9326/aaf2ed14.

Boyer, Syd Levitus, John Antonov, Ricardo Locarnini,1 Alexey Mishonov,Hernan Garcia and Simon A. Josey, (2007), Changes in freshwater content in the North Atlantic Ocean 1955–2006GEOPHYSICAL RESEARCH LETTERS, VOL. 34, L16603, doi:10.1029/2007GL030126, 2007

Broecker, W. S. (1997) ,Thermohaline Circulation, the Achilles Heel of Our Climate System: Will Man-Made CO2 Upset the Current Balance? Science 278,1582-1588.DOI:10.1126/science.278.5343.1582.

Bromwich, D. H., Wilson, A. B., Bai, L., Liu, Z., Barlage, M., Shih, C.-F., Maldonado, S., Hines, K. M., Wang, S.-H., Woollen, J., Kuo, B., Lin, H.-C., Wee, T.-K., Serreze, M. C., and Walsh, J. E.: The Arctic System Reanalysis, Version 2, Bull. Am. Meteorol. Soc., 99, 805–828, https://doi.org/10.1175/BAMS-D-16-0215.1, 2018.

Bulgin, C. E., Thomas, C. M., Waller, J. A., & Woolliams, E. R. (2022). Representation uncertainty in the Earth sciences. Earth and Space Science, 9, e2021EA002129. https://doi.org/10.1029/2021EA002129.

Burchard, H., and Coauthors, 2018: The Knudsen theorem and the Total Exchange Flow analysis framework applied to the Baltic Sea. Prog. Oceanogr. 165, 268–286, https://doi.org/10.1016/j.pocean 2018.04.004.

Carmack, E. C. (2007). The alpha/beta ocean distinction: A perspective on freshwater fluxes, convection, nutrients and productivity in high-latitude seas. Deep Sea Research Part II: Topical Studies in Oceanography, 54(23-26), 2578–2598. 17) Carmack, E. C., Yamamoto-Kawai, M., Haine, T. W., Bacon, S., Bluhm, B. A., & Lique, C. (2016). Freshwater and its role in the Arctic marine system: Sources, disposition, storage, export, and physical and biogeochemical consequences in the Arctic and global oceans. Journal of Geophysical Research: Biogeosciences, 121(3), 675–717.

Carmack, E., et al. (2016). Toward quantifying the increasing role of oceanic heat in sea ice loss in the new Arctic. Bulletin of the American Meteorological Society, 97(12), 2079-2105.

Charkin, A. N., Rutgers van der Loeff, M., Shakhova, N. E., Gustafsson, Ö., Dudarev, O. V., Cherepnev, M. S., Salyuk, A. N., Koshurnikov, A. V., Spivak, E. A., Gunar, A. Y., Ruban, A. S., and Semiletov, I. P. (2017): Discovery and characterization of submarine groundwater discharge in the Siberian Arctic seas: a case study in the Buor-Khaya Gulf, Laptev Sea, The Cryosphere, 11, 2305–2327, https://doi.org/10.5194/tc-11-2305-2017 .

Church, J. A., et al. (2013). Sea level change. In T. F. Stocker et al. (Eds.), Climate Change 2013: The Physical Science Basis. Contribution of Working Group I to the Fifth Assessment Report of the Intergovernmental Panel on Climate Change. Cambridge University Press.

Curry, B., C. M. Lee, B. Petrie, R. E. Moritz, and R. Kwok, 2014: Multiyear Volume, Liquid Freshwater, and Sea Ice Transports through Davis Strait, 2004–10. J. Phys. Oceanogr., 44, 1244–1266, https://doi.org/10.1175/JPO-D-13-0177.1.

Da Silva, E., Woolliams, E. R., Picot, N., Poisson, J.-C., Skourup, H., Moholdt, G., Fleury, S., Behnia, S., Favier, V., & Arnaud, L., et al. (2023). Towards operational fiducial reference measurement (FRM) data for the calibration and validation of the Sentinel-3 surface topography mission over inland waters, sea ice, and land ice. Remote Sensing, 15, 4826. https://doi.org/10.3390/rs15194826

De Andres, E., Umbert, M., Sanchez-Urrea, M., Gonzalez-Gambau, V., Olmedo, E., Gabarro, C., & Elosegui, P. (2023). Sea ice meltwater in the Beaufort gyre: A comprehensive analysis using sea surface salinity data from SMOS. Authorea Preprints.

Dickson, R. R., Meincke, J., Malmberg, S. A., & Lee, A. J. (1988). The “great salinity anomaly” in the northern North Atlantic 1968–1982. Progress in Oceanography, 20(2), 103-151.

Dyurgerov, M., Bring, A., & Destouni, G. (2010). Integrated assessment of changes in freshwater inflow to the Arctic Ocean. Journal of Geophysical Research, 115, D12116. https://doi.org/10.1029/2009JD013060

Enderlin, E. M., Howat, I. M., Jeong, S., Noh, M.-J., van Angelen, J. H., & van den Broeke, M. R. (2014). An improved mass budget for the Greenland ice sheet. Geophysical Research Letters, 41, 866 24.

Fettweis, X., et al. (2020). GrSMBMIP: Intercomparison of the modelled 1980–2012 surface mass balance over the Greenland Ice Sheet. The Cryosphere, 14(11), 3935-3958.

Florindo-López, C., S. Bacon, Y. Aksenov, L. Chafik, E. Colbourne, and N. P. Holliday, 2020: Arctic Ocean and Hudson Bay Freshwater Exports: New Estimates from Seven Decades of Hydrographic Surveys on the Labrador Shelf. *J. Climate*, **33**, 8849–8868, https://doi.org/10.1175/JCLI-D-19-0083.1.

Font, J., Camps, A., Borges, A., Martín-Neira, M., Boutin, J., Reul, N., … Mecklenburg, S. (2010). SMOS: The challenging sea surface salinity measurement from space. Proceedings of the IEEE, 98(5), 649-665. https://doi.org/10.1109/JPROC.2009.2033096

Ford, V. L., & Frauenfeld, O. W. (2022). Arctic precipitation recycling and hydrologic budget changes in response to sea ice loss. Global and Planetary Change, 209, 103752. https://doi.org/10.1016/j.gloplacha.2022.103752

Forryan, A., Bacon, S., Tsubouchi, T., Torres-Valdés, S., & Naveira Garabato, A. C. (2019). Arctic freshwater fluxes: sources, tracer budgets and inconsistencies. The Cryosphere, 13, 2111–2131. https://doi.org/10.5194/tc-13-2111-2019

Forsström, S., Gerland, S., & Pedersen, C. A. (2011). Thickness and density of snow-covered sea ice and hydrostatic equilibrium assumption from in situ measurements in Fram Strait, the Barents Sea and the Svalbard coast. Annals of Glaciology, 52(57), 261-270. https://doi.org/10.3189/172756411795931598

Fournier, S., Lee, T., Wang, X., Armitage, T. W. K., Wang, O., Fukumori, I., & Kwok, R. (2020). Sea surface salinity as a proxy for Arctic Ocean freshwater changes. Journal of Geophysical Research: Oceans, 125, e2020JC016110. https://doi.org/10.1029/2020JC016110

Fukumori, I., Wang, O., & Fenty, I. (2021). Causal mechanisms of sea level and freshwater content change in the Beaufort Sea. Journal of Physical Oceanography, 51(10), 3217–3234. https://doi.org/10.1175/JPO-D-21-0069.1

Gardner, A. S., et al. (2013). A reconciled estimate of glacier contributions to sea level rise: 2003 to 2009. Science, 340, 852- 857. https://doi.org/10.1126/science.1234532

Giles, K. A., Laxon, S. W., Ridout, A. L., Wingham, D. J., & Bacon, S. (2012). Western Arctic Ocean freshwater storage increased by wind-driven spin-up of the Beaufort Gyre. Nature Geoscience, 5(3), 194–197. https://doi.org/10.1038/ngeo1379

Global Climate Observing System (GCOS): The 2022 GCOS Implementation Plan. Technical report, GCOS (2022). https://gcos.wmo.int/en/publications/gcos-implementation-plan2022

Goryl, P., Fox, N., Donlon, C., & Castracane, P. (2023). Fiducial reference measurements (FRMs): What are they? Remote Sensing, 15(20), 5017. https://doi.org/10.3390/rs15205017

Gutenstein, M., Fennig, K., Schröder, M., Trent, T., Bakan, S., Roberts, J. B., & Robertson, F. R. (2021). Intercomparison of freshwater fluxes over ocean and investigations into water budget closure. Hydrology and Earth System Sciences, 25, 121– 146. https://doi.org/10.5194/hess-25-121-2021

Haine, T.W.N., Martin, T. The Arctic-Subarctic sea ice system is entering a seasonal regime: Implications for future Arctic amplification. *Sci Rep* **7**, 4618 (2017). https://doi.org/10.1038/s41598-017-04573-0

Hall, S. B., Subrahmanyam, B., & Morison, J. H. (2022). Intercomparison of salinity products in the Beaufort Gyre and Arctic Ocean. Remote Sensing, 14, 71. https://doi.org/10.3390/rs14010071

Hall, S. B., Subrahmanyam, B., Nyadjro, E. S., & Samuelsen, A. (2021). Surface freshwater fluxes in the Arctic and Subarctic seas during contrasting years of high and low summer sea ice extent. Remote Sensing, 13, 1570. https://doi.org/10.3390/rs13081570

Hall, S. B., Subrahmanyam, B., & Steele, M. (2023). The role of the Russian Shelf in seasonal and interannual variability of Arctic sea surface salinity and freshwater content. Journal of Geophysical Research: Oceans, 128, e2022JC019247. https://doi.org/10.1029/2022JC019247

He, Y., Shu, Q., Wang, Q. *et al.* Arctic Amplification of marine heatwaves under global warming. *Nat Commun* 15, 8265 (2024). https://doi.org/10.1038/s41467-024-52760-1

Haine, T. W. N., Curry, B., Gerdes, R., Hansen, E., Karcher, M., Lee, C., et al. (2015). Arctic freshwater export:

Status, mechanisms, and prospects. Global and Planetary Change, 125, 13–35. https://doi.org/10.1016/J.GLOPLACHA.2014.11.013

Hersbach, H., Bell, B., Berrisford, P., et al. (2020). The ERA5 global reanalysis. Quarterly Journal of the Royal Meteorological Society, 146, 1999–2049. https://doi.org/10.1002/qj.3803

Hiyama, T., Park, H., Kobayashi, K., Lebedeva, L., Gustafsson, D. (2023). Contribution of summer net precipitation to winter river discharge in permafrost zone of the Lena River basin. Journal of Hydrology, 616, 128797, https://doi.org/10.1016/j.jhydrol.2022.128797

Howell, S. E. L., Babb, D. G., Landy, J. C., Moore, G. W. K., Montpetit, B., & Brady, M. (2023). A comparison of Arctic Ocean sea ice export between Nares Strait and the Canadian Arctic Archipelago. Journal of Geophysical Research: Oceans, e2023JC019687.

Howell, S. E. L., Brady, M., & Komarov, A. S. (2022). Generating large-scale sea ice motion from Sentinel-1 and the RADARSAT constellation mission using the environment and climate change Canada automated sea ice tracking system. The Cryosphere, 16(3), 1125–1139. https://doi.org/10.5194/tc-16-1125-2022

Howell, S. E. L., Babb, D. G., Landy, J. C., Moore, G. W. K., Ballinger, T. J., McNeil, K., et al. (2024). Baffin Bay ice export and production from Sentinel-1, the RADARSAT Constellation Mission, and CryoSat-2: 2016–2022. Geophysical Research Letters, 51, e2024GL111364.https://doi.org/10.1029/2024GL111364

Huang, B., Wang, Z., Yin, X., Arguez, A., Graham, G., Liu, C., et al. (2021). Prolonged marine heatwaves in the Arctic: 1982−2020. *Geophysical Research Letters*, 48, e2021GL095590. https://doi.org/10.1029/2021GL095590

Huffman, G. J., Adler, R. F., Morrissey, M. M., Bolvin, D. T., Curtis, S., Joyce, R., McGavock, B., & Susskind, J. (2001). Global precipitation at one-degree daily resolution from multisatellite observations. Journal of Hydrometeorology, 2, 36–50. https://doi.org/10.1175/1525-7541(2001)002<0036:GPAODD>2.0.CO;2

Hugonnet, R., McNabb, R., Berthier, E., et al. (2021). Accelerated global glacier mass loss in the early twenty-first century. Nature, 592, 726–731. https://doi.org/10.1038/s41586-021-03436-z.

IPCC. (2021). Climate Change 2021: The Physical Science Basis. Contribution of Working Group I to the Sixth Assessment Report of the Intergovernmental Panel on Climate Change [Masson-Delmotte, V., et al. (eds.)]. Cambridge University Press. 42) Joint Committee for Guides in Metrology. (2008). Evaluation of measurement data — Guide to the expression of uncertainty in measurement. https://www.bipm.org/documents/20126/2071204/JCGM_100_2008_E.pdf

JCGM 100: Evaluation of measurement data — Guide to the expression of uncertainty in measurement. Guide JCGM 100:2008, BIPM, IEC, IFCC, ILAC, ISO, IUPAC, IUPAP and OIML (2008). https://doi.org/10.59161/JCGM100-2008E.

JCGM 200: International vocabulary of metrology — Basic and general concepts and associated terms. Guide JCGM 200:2012, BIPM, IEC, IFCC, ILAC, ISO, IUPAC, IUPAP and OIML. (2012). https://doi.org/10.59161/JCGM200-2012

JCGM GUM-1: Guide to the expression of uncertainty in measurement — Part 1: Introduction. guide JCGM GUM-1-2023:2023, BIPM, IEC, IFCC, ILAC, ISO, IUPAC, IUPAP and OIML (2023). https://doi.org/10.59161/JCGMGUM-1-2023

Karlsson, N. B., et al. (2023). A data set of monthly freshwater fluxes from the Greenland ice sheet's marine-terminating glaciers on a glacier–basin scale 2010–2020. GEUS Bulletin, 53, 8338.

Karpouzoglou, T., de Steur, L., Smedsrud, L. H., & Sumata, H. (2022). Observed changes in the Arctic freshwater outflow in Fram Strait. Journal of Geophysical Research: Oceans, 127, e2021JC018122. https://doi.org/10.1029/2021JC018122

King, M. D., Howat, I. M., Jeong, S., Noh, M. J., Wouters, B., Noël, B., & van den Broeke, M. R. (2018). Seasonal to decadal variability in ice discharge from the Greenland Ice Sheet. The Cryosphere, 12, 3813–3825. https://doi.org/10.5194/tc-12- 3813-2018

King, M. D., Howat, I. M., Candela, S. G., et al. (2020). Dynamic ice loss from the Greenland Ice Sheet driven by sustained glacier retreat. Communications Earth & Environment, 1, 1. https://doi.org/10.1038/s43247-020-0001-2

Knudsen, M., 1900: Ein hydrographischer Lehrsatz (in German). Ann. Hydrogr. Marit. Meteor., 28 (7), 316–320.

Kolodziejczyk, N., Hamon, M., Boutin, J., Vergely, J.-L., Reverdin, G., Supply, A., & Reul, N. (2021). Objective analysis of SMOS and SMAP sea surface salinity to reduce large-scale and time-dependent biases from low to high latitudes. Journal of Atmospheric and Oceanic Technology, 38(3), 405–421.

Krumpen, T., Gerdes, R., Haas, C., Hendricks, S., Herber, A., Selyuzhenok, V., & Spreen, G. (2016). Recent summer sea ice thickness surveys in Fram Strait and associated ice volume fluxes. The Cryosphere, 10(2), 523-534.

Krumpen, T., von Albedyll, L., Bünger, H.J. et al. (2025), Smoother sea ice with fewer pressure ridges in a more dynamic Arctic. Nat. Clim. Chang. 15, 66–72. https://doi.org/10.1038/s41558-024-02199-5

Kwok, R., & Rothrock, D. A. (1999). Variability of Fram Strait ice flux and North Atlantic oscillation. Journal of Geophysical Research: Oceans, 104(C3), 5177-5189.

Kwok, R., Schweiger, A., Rothrock, D. A., Pang, S., & Kottmeier, C. (1998). Sea ice motion from satellite passive microwave data assessed with ERS SAR and buoy data. Journal of Geophysical Research, 103(C4), 8191–8214. https://doi.org/10.1029/97jc03334

Lagerloef, G., Colomb, F. R., Vine, D. L., Wentz, F., Yueh, S., Ruf, C., & Swift, C. (2008). The Aquarius/SAC-D mission: Designed to meet the salinity remote-sensing challenge. Oceanography, 21(1), 68–81. https://www.jstor.org/stable/24860158 52) Lenaerts, J. T. M., Le Bars, D., Van Kampenhout, L., Vizcaino, M., Enderlin, E. M., & Van Den Broeke, M. R. (2015). Representing Greenland ice sheet freshwater fluxes in climate models. Geophysical Research Letters, 42(15), 6373–6381. https://doi.org/10.1002/2015GL064738

Landy, J. C., Dawson, G. J., Tsamados, M., Bushuk, M., Stroeve, J. C., Howell, S. E. L., et al. (2022). A year-round satellite sea-ice thickness record from CryoSat-2. Nature, 609(7927), 517–522. https://doi.org/10.1038/s41586-022-05058-5

Lebedeva L., Gustafsson D. (2021) Streamflow Changes of Small and Large Rivers in the Aldan River Basin, Eastern Siberia. Water, 13, 2747. https://doi.org/10.3390/w13192747

Le Bras, I. A.-A., & Timmermans, M.-L. (2025). Can the marked Arctic Ocean freshwater content increases of the last two decades be explained within observational uncertainty? Journal of Geophysical Research: Oceans, 130, e2024JC021061.https://doi.org/10.1029/2024JC021061

Lique, C., Treguier, A. M., Scheinert, M., & Penduff, T. (2009). A model-based study of ice and freshwater transport variability along both sides of Greenland. Climate Dynamics, 33, 685-705.

Lique Camille (2015). Arctic sea ice heated from below . *Nature Geoscience* , 8(3), 172-173 . https://doi.org/10.1038/ngeo2357

Loomis, B. D., Luthcke, S. B., & Sabaka, T. J. (2019). Regularization and error characterization of GRACE mascons. Journal of Geodesy, 93(9), 1381–1398. https://doi.org/10.1007/s00190-019-01252-y

Ludwigsen, C. A., & Andersen, O. B. (2021). Contributions to Arctic sea level from 2003 to 2015. Advances in Space Research, 68(2), 703–710. https://doi.org/10.1016/j.asr.2019.12.027.

Nielsen, K. P., Yang, X., Agersten, S., Dahlgren, P., Ødegaard Køltzow, M. A., Schyberg, H., Støylen, E., & Bojarova, J. (2022). Copernicus Arctic Regional Reanalysis (CARRA): Data user guide. https://confluence.ecmwf.int/display/CKB/Copernicus+Arctic+Regional+Reanalysis+%28CARRA%29%3A+Data+User+Guide.

Mankoff, K. D., et al. (2020). Greenland Ice Sheet solid ice discharge from 1986 through March 2020. Earth System Science Data, 12(2), 1367-1383.

Martinez, J., Gabarró, C., Turiel, A., González-Gambau, V., Umbert, M., Hoareau, N., et al. (2022). Improved BEC SMOS Arctic sea surface salinity product v3. 1. Earth System Science Data, 14(1), 307–323.

Matsuoka, A., Babin, M., & Devred, E. C. (2016). A new algorithm for discriminating water sources from space: A case study for the southern Beaufort Sea using MODIS ocean color and SMOS salinity data. Remote Sensing of Environment, 184, 124- 138.

McPhee, M. G., Proshutinsky, A., Morison, J. H., Steele, M., & Alkire, M. B. (2009). Rapid change in freshwater content of the Arctic Ocean. Geophysical Research Letters, 36(10), 1–6. https://doi.org/10.1029/2009GL037525

Mittaz, J., Merchant, C.J., Woolliams, E.R (2019): Applying principles of metrology to historical Earth observations from satellites. Metrologia 56(3), 032002 https://doi.org/10.1088/1681-7575/ab1705

Moore, G. W. K., Howell, S. E. L., Brady, M., McNeil, K., & Xu, X. (2021). Anomalous collapses of Nares Strait ice arches leads to enhanced export of Arctic sea ice. Nature Communications, 12, 1. https://doi.org/10.1038/s41467-020-20314-w 61) Morison, J., et al. (2012). Changing Arctic Ocean freshwater pathways. Nature, 481, 66-70.

Morison, J., Wahr, J., Kwok, R., & Peralta-Ferriz, C. (2007). Recent trends in Arctic Ocean mass distribution revealed by GRACE. Geophysical Research Letters, 34(7), L07602. https://doi.org/10.1029/2006GL029016

Morison, J., Kwok, R., Peralta-Ferriz, C., Alkire, M., Rigor, I., Andersen, R., & Steele, M. (2012). Changing Arctic Ocean freshwater pathways. Nature, 481(7379), 66–70. https://doi.org/10.1038/nature10705

Morlighem, M., Williams, C., Rignot, E., An, L., Arndt, J. E., Bamber, J., Catania, G., Chauché, N., Dowdeswell, J. A., Dorschel, B., Fenty, I., Hogan, K., Howat, I., Hubbard, A., Jakobsson, M., Jordan, T. M., Kjeldsen, K. K., Millan, R., Mayer, L., Mouginot, J., Noël, B., O'Cofaigh, C., Palmer, S. J., Rysgaard, S., Seroussi, H., Siegert, M. J., Slabon, P., Straneo, F., van den Broeke, M. R., Weinrebe, W., Wood, M., & Zinglersen, K. (2017). BedMachine v3: Complete bed topography and ocean bathymetry mapping of Greenland from multi-beam echo sounding combined with mass conservation. Geophysical Research Letters, 44. https://doi.org/10.1002/2017GL074954

Nagler, T., Rott, H., Hetzenecker, M., Wuite, J., & Potin, P. (2015). The Sentinel-1 Mission: New Opportunities for Ice Sheet Observations. Remote Sensing, 7, 9371-9389. https://doi.org/10.3390/rs70709371

Newton, R., Pfirman, S., Tremblay, B., and DeRepentigny, P.: Increasing transnational sea-ice exchange in a changing Arctic Ocean, Earth's Future, 5, 633–647, 2017.

Nghiem, S. V., et al. (2012). The extreme melt across the Greenland ice sheet in 2012. Geophysical Research Letters, 39(20). 66)

Nygard, T., Naakka, T., and Vihma, T.: Horizontal moisture transport dominates the regional moistening patterns in the Arctic, J. Clim., 33, 6793–6807, 2020.

Olmedo, E., Gabarró, C., González-Gambau, V., Martínez, J., Ballabrera-Poy, J., Turiel, A., ... Lee, T. (2018). Seven years of SMOS sea surface salinity at high latitudes: Variability in Arctic and sub-Arctic regions. Remote Sensing, 10(11), 1772. 67) Otosaka, I. N., et al. (2023). Mass balance of the Greenland and Antarctic ice sheets from 1992 to 2020. Earth System Science Data, 15, 1597–1616. https://doi.org/10.5194/essd-15-1597-2023

Parkinson et Comismo (2013), On the 2012 record low Arctic sea ice cover: Combined impact of preconditioning and an August storm. GEOPHYSICAL RESEARCH LETTERS, VOL. 40, 1356–1361, doi:10.1002/grl.50349, 2013.

Paul, S., Hendricks, S., Rinne, E., & Sallila, H. (2024). CCI+ Sea Ice ECV - Sea Ice Thickness Algorithm Theoretical Basis Document (ATBD) (3.2). Zenodo. https://doi.org/10.5281/zenodo.10605840

Peralta-Ferriz, C., & Morison, J. (2010). Understanding the Arctic freshwater budget: Capabilities of current models and data. Reviews of Geophysics, 48, RG4002.

Peralta-Ferriz, C., & Woodgate, R. A. (2015). Seasonal and interannual variability of pan-Arctic surface mixed layer properties from 1979 to 2012 from hydrographic data, and the dominance of stratification for multiyear mixed layer depth shoaling. Progress in Oceanography, 134, 19-53.

Peralta-Ferriz, C., & Woodgate, R. A. (2023). Arctic and sub-Arctic mechanisms explaining observed increasing northward flow through the Bering Strait and why models may be getting it wrong. Geophysical Research Letters, 50, e2023GL104697. https://doi.org/10.1029/2023GL104697

Peralta-Ferriz, C., Morison, J. H., Wallace, J. M., Bonin, J. A., & Zhang, J. (2014). Arctic ocean circulation patterns revealed by GRACE. Journal of Climate, 27(4), 1445–1468. https://doi.org/10.1175/JCLI-D-13-00013.1

Petty, A. A., et al. (2018). The Arctic sea ice cover of 2016: A year of record-low highs and higher-than-expected lows. The Cryosphere, 12(2), 433-452.

Piepmeier, J. R., Focardi, P., Horgan, K. A., Knuble, J., Ehsan, N., Lucey, J., ... Njoku, E. G. (2017). SMAP L-band microwave radiometer: Instrument design and first year on orbit. IEEE Transactions on Geoscience and Remote Sensing, 55(4), 1954- 1966. https://doi.org/10.1109/TGRS.2016.2631978

Polyakov, I. V., et al. (2020). Weakening of cold halocline layer exposes sea ice to oceanic heat in the eastern Arctic Ocean. Journal of Climate, 33(18), 8107-8123.

Polyakov, I. V *et al.,* (2023) Fluctuating Atlantic inflows modulate Arctic atlantification.*Science***381**,972-979. DOI:10.1126/science.adh5158

Proshutinsky, A., Krishfield, R., Timmermans, M.-L., Toole, J., Carmack, E., McLaughlin, F., et al. (2009). Beaufort Gyre freshwater reservoir: State and variability from observations. Journal of Geophysical Research, 114(C1), C00A10. https://doi.org/10.1029/2008JC005104

Proshutinsky, A., Krishfield, R., Toole, J. M., Timmermans, M. L., Williams, W., Zimmermann, S., et al. (2019). Analysis of the Beaufort Gyre freshwater content in 2003-2018. Journal of Geophysical Research: Oceans, 124(12), 1–32. https://doi.org/10.1029/2019JC015281

Prowse, T., A. Bring, J. Mård, E. Carmack, M. Holland, A. Instanes, T. Vihma, and F. J. Wrona (2015), Arctic Freshwater Synthesis: Summary of key emerging issues, J. Geophys. Res. Biogeosci., 120, 2121–2131, doi:10.1002/2015JG003128.

Rabe, B., Karcher, M., Kauker, F., Schauer, U., Toole, J. M., Krishfield, R. A., Pisarev, S., Kikuchi, T., & Su, J. (2014). Arctic Ocean Basin Liquid Freshwater Storage Trend 1992–2012. Geophysical Research Letters, 41, 961–968.

Rahmstorf, S., et al. (2015). Exceptional twentieth-century slowdown in Atlantic Ocean overturning circulation. Nature Climate Change, 5(5), 475-480.

Rantanen, M., Karpechko, A.Y., Lipponen, A. *et al.* The Arctic has warmed nearly four times faster than the globe since 1979. *Commun Earth Environ* **3**, 168 (2022). https://doi.org/10.1038/s43247-022-00498-3

Richaud, B., Hu, X., Darmaraki, S., Fennel, K., Lu, Y., & Oliver, E. C. J. (2024). Drivers of marine heatwaves in the Arctic Ocean. *Journal of Geophysical Research: Oceans*, 129, e2023JC020324. https://doi.org/10.1029/2023JC020324

Ricker, R., Girard-Ardhuin, F., Krumpen, T., & Lique, C. (2018). Satellite-derived sea ice export and its impact on Arctic ice mass balance. The Cryosphere, 12(9), 3017-3032.

Ricker, R., Kauker, F., Schweiger, A., Hendricks, S., Zhang, J., & Paul, S. (2021). Evidence for an increasing role of ocean heat in Arctic winter sea ice growth. Journal of Climate, 34(13), 5215-5227.

Rose, S. K., Andersen, O. B., Passaro, M., Ludwigsen, C. A., & Schwatke, C. (2019). Arctic Ocean Sea Level Record from the Complete Radar Altimetry Era: 1991–2018. Remote Sensing, 11, 1672. https://doi.org/10.3390/rs11141672

Sakov, P., Counillon, F., Bertino, L., Lisaeter, K. A., Oke, P. R., Korablev, A. (2012). TOPAZ4: an ocean-sea ice data assimilation system for the North Atlantic and Arctic. Ocean Science, 8, 633–656. https://doi.org/10.5194/os-8-633-2012 81) Screen, J. A., & Simmonds, I. (2010). The central role of diminishing sea ice in recent Arctic temperature amplification. Nature, 464(7293), 1334-1337.

Schauerer, U. and M. Laush.,(2019) : ‘’Freshwater’’ in the Ocean is Not a Useful Parameter in Climate Research. Journal of Physical Oceanography, 49, 2309-2322, DOI: 10.1175/JPO-D-19-0102.1.

Selyuzhenok, V., Bashmachnikov, I., Ricker, R., Vesman, A., and Bobylev, L. (2020): Sea ice volume variability and water temperature in the Greenland Sea, The Cryosphere, 14, 477–495, https://doi.org/10.5194/tc-14-477-2020.

Serreze, M. C., & Barry, R. G. (2011). Processes and impacts of Arctic amplification: A research synthesis. Global and Planetary Change, 77(1-2), 85-96.

Shiklomanov, A., Déry, S., Tretiakov, M., Yang, D., Magritsky, D., Georgiadi , A., Tang, W. (2021). River Freshwater Flux to the Arctic Ocean. In: Yang, D., Kane, D.L. (eds) Arctic Hydrology, Permafrost and Ecosystems. Springer, Cham. https://doi.org/10.1007/978-3-030-50930-9_24.

Skagseth, Ø. (2008). Recirculation of Atlantic water in the western Barents Sea. Geophysical Research Letters, 35(11).

Smedsrud, L. H., Halvorsen, M. H., Stroeve, J. C., Zhang, R., and Kloster, K., 2017: Fram Strait sea ice export variability and September Arctic sea ice extent over the last 80 years, The Cryosphere, 11, 65–79, https://doi.org/10.5194/tc-11-65-2017

Solomon, A., Heuzé, C., Rabe, B., Bacon, S., Bertino, L., Heimbach, P., Inoue, J., Iovino, D., Mottram, R., Zhang, X., Aksenov, Y., McAdam, R., Nguyen, A., Raj, R. P., & Tang, H. (2021). Freshwater in the Arctic Ocean 2010–2019. Ocean Science, 17, 1081– 1102. https://doi.org/10.5194/os-17-1081-2021

Sommer, C., Seehaus, T., Glazovsky, A., & Braun, M. H. (2022). Brief communication: Increased glacier mass loss in the Russian High Arctic (2010–2017). The Cryosphere, 16, 35–42. https://doi.org/10.5194/tc-16-35-2022

Serreze, M. C., Barrett, A. P., Slater, A. G., Woodgate, R. A., Aagaard, K., Lammers, R. B., et al. (2006). The large-scale freshwater cycle of the Arctic. Journal of Geophysical Research, 111(C11). https://doi.org/10.1029/2005JC003424

Spreen, G., de Steur, L., Divine, D., Gerland, S., Hansen, E., & Kwok, R. (2020). Arctic sea ice volume export through Fram Strait from 1992 to 2014. Journal of Geophysical Research: Oceans, 125(6), e2019JC016039.

Stern, H. L. (2025). Regime shift in Arctic Ocean sea-ice extent. *Geophysical Research Letters*, 52, e2024GL114546. https://doi.org/10.1029/2024GL114546

Strobl, P., Woolliams, E., Molch, K. (submitted Dec 2023). Lost in translation, The need for common vocabularies and an interoperable thesaurus in Earth sciences. Surveys in Geophysics. (Under peer review).

Stroeve, J., D. Notz (2018), Changing state of Arctic sea ice across all seasons. Environ. Res. Lett. 13, 10300.

Sumata, H., Gerdes, R., Kauker, F., and Karcher, M. (2015): Empirical error functions for monthly mean Arctic sea- ice drift, J. Geophys. Res.-Oceans, 120, 7450–7475, https://doi.org/10.1002/2015JC011151.

Sumata, H., de Steur, L., Gerland, S., Divine, D. V., & Pavlova, O. (2022). Unprecedented decline of Arctic sea ice outflow in 2018. Nature Communications, 13(1), 1747.https://doi.org/10.1038/s41467-022-29470-7

Sumata, H., de Steur, L., Divine, D.V. *et al.* Regime shift in Arctic Ocean sea ice thickness. *Nature* **615**, 443–449 (2023). https://doi.org/10.1038/s41586-022-05686-x

Supply, A., Boutin, J., Kolodziejczyk, N., Reverdin, G., Lique, C., Vergely, J.-L., & Perrot, X. (2022). Meltwater lenses over the Chukchi and the Beaufort seas during summer 2019: From in situ to synoptic view. Journal of Geophysical Research: Oceans, 127(12), e2021JC018388.

Supply, A., Boutin, J., Vergely, J.-L., Kolodziejczyk, N., Reverdin, G., Reul, N., & Tarasenko, A. (2020). New insights into smos sea surface salinity retrievals in the arctic ocean. Remote sensing of environment, 249 , 112027.

Tajouri, S., Llovel, W., Sévellec, F., Molines, J.-M., Mathiot, P., Penduff, T., & Leroux, S. (2024). Simulated impact of time-varying river runoff and Greenland freshwater discharge on sea level variability in the Beaufort Gyre over 2005–2018. *Journal of Geophysical Research: Oceans*, 129, e2024JC021237. https://doi.org/10.1029/2024JC021237.

Tang, W., Yueh, S., Yang, D., Fore, A., Hayashi, A., Lee, T., ... & Holt, B. (2018). The potential and challenges of using soil moisture active passive (SMAP) sea surface salinity to monitor Arctic ocean freshwater changes. Remote Sensing, 10(6), 869.

Tarasenko, A., Supply, A., Kusse-Tiuz, N., Ivanov, V., Makhotin, M., Tournadre, J., Chaperon, Kolodziejczyk, N., & Reverdin, G. (2021). Properties of surface water masses in the Laptev and the East Siberian seas in summer 2018 from in situ and satellite data. Ocean Science, 17(1), 221–247.

The GlaMBIE Team. Community estimate of global glacier mass changes from 2000 to 2023. *Nature* **639**, 382–388 (2025). https://doi.org/10.1038/s41586-024-08545-z

Trusel, L. D., Das, S. B., Osman, M. B., Evans, M. J., Smith, B. E., Fettweis, X., ... & van den Broeke, M. R. (2018). Nonlinear rise in Greenland runoff in response to post-industrial Arctic warming. Nature, 564(7734), 104–108.

Tsubouchi, T., Bacon, S., Aksenov, Y., Garabato, A. C. N., Beszczynska-Möller, A., Hansen, E., ... & Lee, C. M. (2018). The Arctic ocean seasonal cycles of heat and freshwater fluxes: Observation-based inverse estimates. Journal of Physical Oceanography, 48(9), 2029–2055.

Tsubouchi, T., Bacon, S., Naveira Garabato, A. C., Aksenov, Y., Laxon, S. W., Fahrbach, E., et al. (2012). The Arctic Ocean in summer: A quasi-synoptic inverse estimate of boundary fluxes and water mass transformation. Journal of Geophysical Research, 117(1), 1–28. https://doi.org/10.1029/2011JC007174

Tsubouchi, T., von Appen, W.-J., Kanzow, T., & de Steur, L. (2023). Temporal variability of the overturning circulation in the Arctic Ocean and the associated heat and freshwater transports during 2004-2010. Journal of Physical Oceanography, 1(aop). https://doi.org/10.1175/JPO-D-23-0056.1

Van Den Broeke, M. R., Enderlin, E. M., Howat, I. M., Kuipers Munneke, P., Noël, B. P. Y., Jan Van De Berg, W., ... & Wouters, B. (2016). On the recent contribution of the Greenland ice sheet to sea level change. The Cryosphere, 10(5), 1933–1946. 95) Vinje, T. (2001). Fram Strait ice fluxes and atmospheric circulation: 1950–2000. Journal of Climate, 14(16), 3508-3517. 96)

Van Straaten, C., Lique, C., & Kolodziejcyk, N. (2025). The life cycle of the low salinity lenses at the surface of the Arctic Ocean. *Journal of Geophysical Research: Oceans*, 130, e2024JC021699. https://doi.org/10.1029/2024JC021699

Volkov, V. A., Mushta, A., and Demchev, D.: Sea Ice Drift in the Arctic, in: Sea Ice in the Arctic, Springer, Cham, 301–313, 2020.

Wang, S., Wang, Q., Shu, Q., Song, Z., Lohmann, G., Danilov, S., & Qiao, F. (2021). Nonmonotonic change of the Arctic Ocean freshwater storage capability in a warming climate. Geophysical Research Letters, 48(10), e2020GL090951. https://doi.org/10.1029/2020gl090951

Wang, S., Wang, Q., Wang, M., Lohmann, G., & Qiao, F. (2022). Arctic Ocean freshwater in CMIP6 coupled models. Earth's Future, 10, e2022EF002878. https://doi.org/10.1029/2022EF002878

Wake, L. M., Lecavalier, B. S., & Bevis, M. (2016). Glacial Isostatic Adjustment (GIA) in Greenland: a Review. Current Climate Change Reports, 2(3), 101–111.

Warren, S. G., Rigor, I. G., Untersteiner, N., Radionov, V. F., Bryazgin, N. N., Aleksandrov, Y. I., & Colony, R. (1999). Snow Depth on Arctic Sea Ice. Journal of Climate, 12, 1814–1829.

Wiese, D. N., Landerer, F. W., & Watkins, M. M. (2016). Quantifying and reducing leakage errors in the JPL RL05M GRACE mascon solution. Water Resources Research, 52, 7490–7502.

Woodgate, R. A., & Aagaard, K. (2005). Revising the Bering Strait freshwater flux into the Arctic Ocean. Geophysical Research Letters, 32, L02602.

Woodgate, R. A. (2018), Increases in the Pacific inflow to the Arctic from 1990 to 2015, and insights into seasonal trends and driving mechanisms from year-round Bering Strait mooring data. Progress in Oceanography, 160, 124–154.

Woodgate, R.A., K.M. Stafford, and F.G. Prahl. (2015), A synthesis of year-round interdisciplinary mooring measurements in the Bering Strait (1990–2014) and the RUSALCA years (2004–2011). Oceanography 28(3):46–67, https://doi.org/10.5670/oceanog.2015.57

Woolliams, E.R., et al. (2025), A metrological framework for addressing uncertainty in satellite and in situ Earth environmental observations, Submitted to Surveys in Geophysics.

Wuite, J., Rott, H., Hetzenecker, M., Floricioiu, D., De Rydt, J., Gudmundsson, G. H., Nagler, T., & Kern, M. (2015). Evolution of surface velocities and ice discharge of Larsen B outlet glaciers from 1995 to 2013. The Cryosphere, 9, 957–969. 102) Xie, J., Bertino, L., Counillon, F., Lisæter, K. A., & Sakov, P. (2017). Quality assessment of the TOPAZ4 reanalysis in the Arctic over the period 1991–2013. Ocean Science, 13(1), 123–144.

Yamazaki, D., O'Loughlin, F., Trigg, M. A., Miller, Z. F., Pavelsky, T. M., & Bates, P. D. (2014). Development of the Global Width Database for Large Rivers.

Zheng, W., Pritchard, M. E., Willis, M. J., Tepes, P., Gourmelen, N., Benham, T. J., & Dowdeswell, J. A. (2018). Accelerating glacier mass loss on Franz Josef Land, Russian Arctic. Remote Sensing of Environment, 211, 357-375. https://doi.org/10.1016/j.rse.2018.04.004.

Zhou, L., Stroeve, J., Xu, S., Petty, A., Tilling, R., Winstrup, M., Rostosky, P., Lawrence, I. R., Liston, G. E., Ridout, A., Tsamados, M., and Nandan, V. (2021): Inter-comparison of snow depth over Arctic sea ice from reanalysis reconstructions and satellite retrieval, The Cryosphere, 15, 345–367, https://doi.org/10.5194/tc-15-345-2021.